

COMPARATIVE ANALYSIS OF URBAN WETLAND CLASSIFICATION
FROM MULTISPECTRAL, HYPERSPECTRAL, AND
FUSED SATELLITE IMAGERY

A THESIS IN
Environmental and Urban Geosciences

Presented to the Faculty of the University
of Missouri-Kansas City in partial fulfillment of
the requirement for the degree

MASTER OF SCIENCE

By

DANIEL WARD GWARTNEY

B.S., University of Kansas, 2006

Kansas City, Missouri
2012

© 2012

DANIEL WARD GWARTNEY

ALL RIGHTS RESERVED

COMPARATIVE ANALYSIS OF URBAN WETLAND CLASSIFICATION
FROM MULTISPECTRAL, HYPERSPECTRAL, AND
FUSED SATELLITE IMAGERY

Daniel Ward Gwartney, Candidate for the Master of Science Degree

University of Missouri-Kansas City, 2012

ABSTRACT

Protection and inventory of current wetlands is important for critical habitats, education, recreation, flood control, and storm water filtration. Over the years, the United States has lost over one-half of its wetlands due to natural processes and urban development. Satellite imagery was used to test the possibility of accurately mapping existing wetlands located in a subset study site along the confluence of the Missouri River and the Blue River in Kansas City, Missouri, following the National Wetlands Inventory (NWI) classification scheme. Testing was performed using hyperspectral (Hyperion) and higher spatial resolution multispectral (SPOT 5) imagery. Additionally, testing was performed by fusing the hyperspectral with multispectral imagery. Results indicated that the fused imagery produced a classified landscape with higher overall accuracy, as well as increased accuracy within the individual wetland classes. These

results are significant because they indicate the possibility of an inexpensive, accurate approach for classifying wetlands to obtain metrics for wetlands within even larger study areas.

APPROVAL PAGE

The faculty listed below, appointed by the Dean of the College of Arts and Sciences have examined a thesis titled “Comparative Analysis of Urban Wetland Classification from Multispectral, Hyperspectral, and Fused Satellite Imagery,” presented by Daniel W. Gwartney, candidate for the Master of Science degree, and certify that in their opinion it is worthy of acceptance.

Supervisory Committee

Wei Ji, Ph.D., Committee Chair
Department of Geosciences

Jejung Lee, Ph.D.
Department of Geosciences

Jim Murrowchick, Ph.D.
Department of Geosciences

CONTENTS

ABSTRACT	iii
LIST OF ILLUSTRATIONS	viii
LIST OF TABLES	x
LIST OF EQUATIONS	xi
ACKNOWLEDGEMENTS	xii
Chapter	
1. INTRODUCTION	1
2. LITERATURE REVIEW	6
3. STUDY SITE	21
4. METHODOLOGY	25
Earth Observing 1 / Hyperion Imagery	25
SPOT 5 Imagery Specifications	27
Atmospheric Correction	29
Geometric Correction	32
Hyperspectral Imagery Sharpening	34
Hyperspectral Derivative Processing	40
Signature Extraction	43
Hyperspectral Dimensionality Reduction	49
Classification	50
Metrics	59

5. RESULTS	68
Hyperion Accuracy	69
SPOT 5 Accuracy	72
PCT Fused (Sharpened) Accuracy	75
Metrics	79
6. SUMMARY AND CONCLUSION	95
Recommendations for Further Research	97
Appendix	
A: Accuracy Assessment Tables	100
B: Land Cover Classification Maps	104
REFERENCE LIST	108
VITA	112

ILLUSTRATIONS

Figure	Page
1. Spectral Overlap between Wetland Types	10
2. Relationship Between Patch Density and Scale	17
3. Shannon Diversity Results for Tide Open and Tide Restricted Wetlands	19
4. Kansas City, MO National Land Cover Database (2001)	23
5. Study Site Location	24
6. Raw Hyperion Imagery Subset	27
7. Raw SPOT 5 Imagery Subset	29
8. DN and Reflectance Profiles for Vegetation	32
9. Geometrically Corrected Hyperion and SPOT 5 Imagery	34
10. 30m Hyperion Imagery Study Area Subset	35
11. 10m SPOT 5 Imagery Study Area Subset	36
12. CN Sharpening Result with Spectral Profile	38
13. Raw, PCT, and GST Imagery Statistics	39
14. Raw Hyperion and PCT Comparison	40
15. 30m Hyperion Derivative Profile	42
16. PCT Fused Derivative Profile	42
17. Hyperion Spectral Library Reflectance	45
18. SPOT 5 Spectral Library Reflectance	46
19. Raw Hyperion Derivative Spectral Library	47
20. PCT Fused Spectral Library	48

ILLUSTRATIONS

Figure	Page
21. SPOT 5 NDVI Vegetation / Non-Vegetation Threshold	52
22. SAM Conceptual Reference	54
23. Raw Hyperion Riverine MF Divided by SAM Result	55
24. Raw Hyperion Riverine MF Divided by SAM Histogram	56
25. Raw Hyperion Riverine MF Divided by SAM Histogram Threshold Result	57
26. Hyperion, PCT Fused, and SPOT 5 Land Cover	58
27. Four-neighbor and Eight-neighbor Patch Differences	60
28. Class Area Distribution per Dataset	82
29. Riverine Classification Comparison	83
30. Impervious Classification Comparison	87
31. Number of Patches Distribution per Dataset	89
32. Hyperion Number of Patches and Largest Patch Index per Class Comparison	90
33. SPOT 5 Number of Patches and Largest Patch Index per Class Comparison	91
34. PCT Fused Number of Patches and Largest Patch Index per Class Comparison	92

TABLES

Table	Page
1. Wetland Inventory Comparison, Blue River Watershed	7
2. Wetland Inventory Comparison, Rock Creek Watershed	8
3. SPOT 5 Spatial and Spectral Resolution	28
4. Hyperion 30m Class Accuracy	70
5. Hyperion 30m Producer / User Accuracy	71
6. SPOT 5 10m Class Accuracy	73
7. SPOT 5 10m Producer / User Accuracy	75
8. PCT Fused (Sharpened) 10m Hyperspectral Class Accuracy	77
9. PCT Fused 10m Hyperspectral Producer / User Accuracy	79
10. Class Area Distribution	81
11. Number of Patches and Largest Patch Index Distributions	86

EQUATIONS

Equation	Page
1. SPOT 5 Calibration to Radiance	30
2. First Derivative	41
3. Normalized Difference Vegetation Index	51
4. Total Class Area with units of Hectares	61
5. Percent of Landscape	62
6. Total Area with units of Hectares	62
7. Class Level Largest Patch Index Percent	64
8. Landscape Level Largest Patch Index Percent	64
9. Shannon's Diversity Index	65
10. Shannon's Evenness Index	66
11. Contagion	67
12. Correlation Between Arrays X and Y	93

ACKNOWLEDGEMENTS

I would like to take the time to thank my wife for supporting me during all of my studies, my children for their patience and understanding while I was working, and my supervisors for understanding my commitment to both work and education as I worked through my thesis research. Additionally, I am grateful for the suggestions and editing assistance provided by Mike Wood as I worked through each chapter of my thesis.

I would like to thank the members of my thesis graduate committee Professor Wei Ji, Professor Jejung Lee, and Professor James Murowchick of UMKC's Department of Geosciences for their support, suggestions, and guidance during this process.

Additionally, I would like to extend a special thank you to Professor Wei Ji for his understanding of both my employment and educational obligations, as well as for working with me remotely when necessary and making time to meet with me throughout the duration of work. Regarding advanced hyperspectral analysis methodology, I am extremely grateful for the support from Brian Collins' (IntTerra, Denver Colorado) as well as for basic IDL codes he provided to assist my research.

Finally, I would like to thank everyone who has taken the time to listen, read, or discuss my research with me over the years.

CHAPTER 1

INTRODUCTION

The diverse nature of wetland areas is an important aspect of the communities and rural areas which they affect. By definition, wetlands are essentially areas of land that are periodically covered with water seasonally, annually, or for very long periods of time. There are numerous functions of wetland environments from providing critical habitats for many species (including birds and aquatic life), to simply being used for recreational reasons. Though some say that wetlands are obstructive to urban development, wetlands are essential not only to species habitat but also for human development to thrive. Wetlands have economic importance when considering wildlife and fish, pollution filtration, coastal erosion prevention, and management of storm water runoff. Prior to this recognition, the United States lost over half of its natural wetlands due to both natural causes and urban development.

Industrial development is very prosperous in areas that have close access to water. This is seen as a good reason for development to take place in and around wetland areas. Of course, with the intrusion of urban environments within wetland areas may drastically alter the characteristics of the environment. Urban wetland habitats "... are often subject to different climate and air quality than nonurban systems." (Windham, Laska, and Wollenberg, 2004) Primary examples include sewage drainage and other toxicants, warmer temperatures due to the proximity of surrounding urban environments, and a decline in wind speed through the wetland environment. Only recently have the

economic importance, as well as the importance to species habitat, come to light in wetland areas. As reported by Karen Rouse of the Missouri Department of Natural Resources, “smaller urban wetlands may be more valuable than rural wetlands to their developed watersheds for water quality improvement and flood retention.” (Rouse, 2004) She goes on to report that “research showed that the closer a wetland resided to the urban growth boundary, the more likely it was to be impacted or removed.” (Rouse, 2004) Measures have been taken to protect water bodies from further obstruction due to development of urban areas. Such measures include awareness groups, functions, or legislation. “The U.S. Federal Wild and Scenic Rivers Act of 1968 established a system to protect wild and scenic rivers from development.” (Enger and Smith, 2004) Section 404 of the Clean Water Act prohibits the filling or draining of wetland/water features for the purpose of development. Despite this, Section 404 and many other forms of legislation do not solely represent wetlands and their diverse nature but rather touches on them.

Many wetlands are on privately owned land, thus becoming the land owner’s responsibility to maintain. Furthermore, the government will only protect those wetlands that are considered jurisdictional; in other words, the government is aware of their existence and takes measures to protect them. As urban areas upstream of wetland environments expand due to urban sprawl, it can be assumed that even without direct invasion, urban growth will still have a negative effect. “Current information on the uplands surrounding wetlands is important because land use practices in uplands cause loss of wetland functions, goods, services and values.” (Ozesmi and Bauer, 2002) This

added stress will then lead to degradation of habitat heterogeneity within the downstream wetland areas.

The desired outcome from governmental regulations in lost wetlands is that they must be replaced elsewhere in an effort to mitigate lost habitats or environmental functions. “In the United States, federal and state regulatory programs require mitigation or compensation for certain types of disturbances... with the ultimate goal of retaining or restoring the ecosystem services provided by aquatic habitat.” (Windham, Laska, and Wollenberg, 2004) This is not totally efficient, however, but there are reasons why this is important in urban areas:

Urban wetlands, although subjected to many disturbances, still provide many functions which make their restoration important. These include provision of habitat for commercially important fish and wildlife species and recreational, educational and aesthetic values which are particularly important given that little natural habitat is available in cities. (Grayson, Chapman, and Underwood, 1998)

Furthermore, they filter toxic wastes, excess nutrients, and other pollutants, prevent erosion, and manage storm waters to reduce gross loss from large flooding events:

However, despite the no-net-loss requirements of the federal Clean Water Act and the restoration components of CERCLA (the Comprehensive Environmental Response, Compensation, and Liability Act, also known as Superfund) and RCRA (the Resource Conservation and Recovery Act), wetlands are still being lost at a significant rate (NRC, 2001), and no metrics are being collected universally to demonstrate the contribution of restored wetlands to larger ecosystem and landscape functions. (Windham, Laska, and Wollenberg, 2004)

Using the theory that the restoration projects taking place for lost wetlands is not fully efficient, we can look at the function of natural wetlands versus the function of restored wetlands. The natural wetland area may be required to support indigenous

species of plants, birds, etc. Once it is seen that wetland areas need to be restored, human alterations to the landscape may change the original function. It may be seen by the land use planner that the new wetland function may be primarily needed for flood or pollution control rather than species habitat. This may allow the introduction of invasive biologic species outcompeting species that may have existed in the original habitat. This is not purely efficient, because it is still harming the natural function that the wetland had recently held. For example, common reed / *Phragmites australis* (*P. australis*), is a very persistent form of invasive plant species in wetland areas. “The common reed flattens the marsh surface, lowers the water table and the salinity of the soil and converts mosaics of vegetation into dense monotypic stands.” (McClary, 2004) Urban developments may even be at fault for the intrusion of such invasive species as common reed. He goes on to state that “...drainage or mosquito ditches, and construction creating higher grounds such as roads have been found to be associated with invasions of *P. australis*.” (McClary, 2004) Because of the effect common reed has on the ecology of the area, it may be altering the natural habitat required for indigenous species to thrive. Despite this, “small, restored, and constructed wetlands in an urban watershed setting may play a significant role in maintaining or improving water quality at the landscape scale.” (Rouse, 2004) Regardless of a wetland’s current or updated function, any wetland is far better than no wetland at all.

Aerial photography or other very high resolution imagery such as IKONOS or Quickbird is commonly accepted platforms used for digitizing wetland coverage. Regarding automated wetland delineation, there are limitations within these platforms.

Detailed spectral information is often lost when using such datasets. Many studies have found that separating different wetland classifications is often extremely difficult if spectral information is not a key component of the data used. With the use of hyperspectral imagery, “training sites for species and communities with unique spectral characteristics (especially exotic species) can be selected and results with very good accuracy have been obtained.” (Jollineau and Howarth, 2008)

The goal of this research is to utilize satellite based hyperspectral imagery to classify wetland features with greater accuracy than conventional satellite imaging sensors. Additional analysis was performed to perform image fusion between SPOT and Hyperion datasets, thus emphasizing the benefits of higher spatial and spectral resolution. Furthermore, an attempt will be made to display the capability of advanced image processing for updating NWI datasets. The United States Geological Survey (USGS) Earth Observer (EO)-1 Hyperion sensor has a very similar spectral resolution to that of most aerial hyperspectral scanners, but has a much lower spatial resolution of 30m. However, this gives the sensor the capability of imaging a much wider swath width and length than possible with aerial hyperspectral imagery at a reduced cost.

CHAPTER 2

LITERATURE REVIEW

The U.S. Fish and Wildlife Service supplies very much outdated NWI maps and datasets, where the data portrayed is mostly derived from airborne photography and site visits. Furthermore, these maps represent wetland features from the mid to late 1980's. Kansas City urban buildup had increased by 10.54% from 8.65% in 1972 to 19.19% in 2001 (Ji, 2008); therefore, it is necessary for these inventories to be updated. The study by Rouse (2004) illustrates the difference between the 1985 NWI dataset and the 2002 inventory of wetlands within the East Fork Little Blue River and Rock Creek Watersheds in Kansas City, Mo (Tables 1 and 2).

Table 1

Wetland Inventory Comparison, Blue River Watershed (Rouse, 2004)

Wetland Type	NWI, 1984/85 (acres)	2002 Inventory (acres)
Lacustrine -- Aquatic Bottom	1	0
Lacustrine -- Unconsolidated Bottom	1,234	1,965
Palustrine -- Aquatic Bed	1	28
Palustrine -- Emergent	58	42
Palustrine -- Forested	162	9
Palustrine -- Scrub Shrub	3	0
Palustrine -- Unconsolidated Bottom	152	181
Total	1,611	2,225

Table 2

Wetland Inventory Comparison, Rock Creek Watershed (Rouse, 2004)

Wetland Type	NWI, 1984/85 (acres)	2002 Inventory (acres)
Riverine – Unconsolidated Shore	4	1
Riverine – Unconsolidated Bottom	54	31
Palustrine – Aquatic Bed	0	0
Palustrine -- Emergent	13	3
Palustrine -- Forested	198	205
Palustrine -- Scrub Shrub	22	20
Palustrine -- Unconsolidated Bottom	72	60
Total	363	320

The Rock Creek Watershed clearly shows a net loss of wetland acreage from 1984 to 2002. Despite the net gain in wetland acreage in the Blue River Watershed, it is clear that particular categories have shown a net loss; the most drastic loss being in forested wetlands. Analyzing satellite imagery for wetland mapping is now becoming more practical than utilizing aerial photographs as was done with the previous NWI data. Relatively large or dispersed study sites may be difficult to efficiently monitor. Despite this, “It is difficult to distinguish between various kinds of marsh surface types using traditional remote sensing technologies like aerial photography interpretations.” (Artigas and Yang, 2004) This is likely due to characteristics such as pitch, roll, and yaw of the

aircraft, ultimately yielding to distortion of the final photograph. Furthermore, it takes a tremendous amount of time to search through large and small areas alike while digitizing all relevant features. Fuller, Morgan, and Aichele reports:

Although the study area was relatively small, and a manual digitizing approach was possible, an automated technique was sought because field-based wetland delineation is labor intensive and costly, whereas a remote sensing approach using high-resolution multispectral satellite imagery can be more cost-and labor-efficient. (Fuller, Morgan, and Aichele, 2006)

The use of modern digital image processing methods to determine surface characteristics are ideal in this situation.

Orbiting satellite imagery, such as Landsat Thematic Mapper and Multispectral Scanner (MSS), provides very useful data in landscape classification with great accuracy. Since the imagery from Landsat MSS is gathered across a wide range of the electromagnetic spectrum from blue to thermal, very detailed landscape classifications are easily made. “For mapping and monitoring large geographic areas, analysis of satellite images is less costly and time-consuming when compared to visual interpretation of aerial photographs.” (Jollineau and Howarth, 2008) Results from the study by Townsend and Walsh (2001) on mapping forested wetlands with Landsat TM data showed relatively high accuracy for particular forested wetland tree species.

Despite the relative accuracy in classification from these systems, the large range of spectral signatures covered by the limited number of spectral bands may not yield as much information as needed for an urban wetland environment. Spectrally similar objects often may be misclassified, thus increasing the margin of error in classification and landscape metrics computations. This is of utmost importance to urban wetlands due

to the relative lack of homogeneity, and some confusion may exist within urban features. Ozesmi and Bauer (2002) show an example of spectral overlap inherent within different wetland types in the near infrared and red bands (Figure 1).

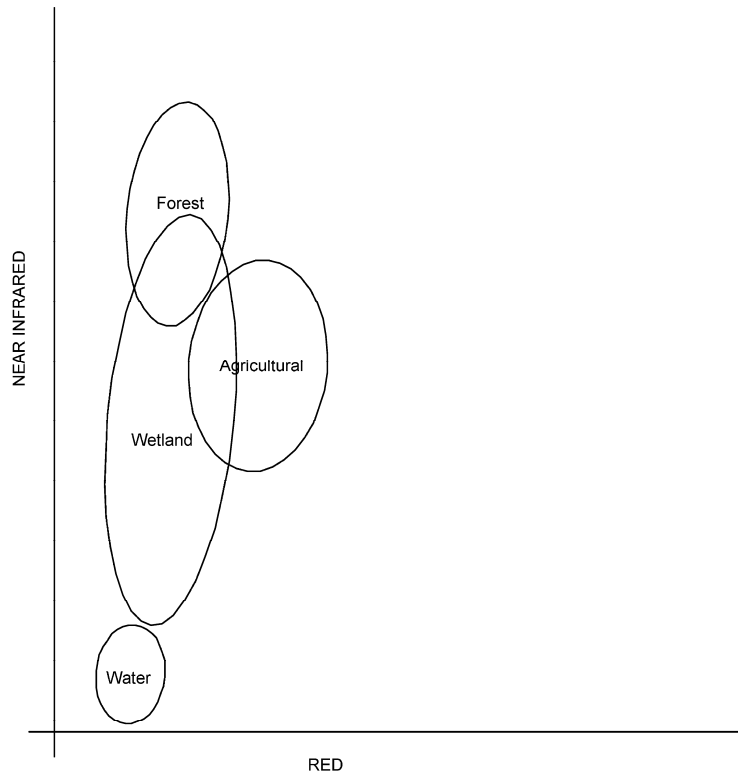


Figure 1. Spectral Overlap between Wetland Types (Ozesmi and Bauer, 2002)

Results from the study by Fuller, Morgan and Aichele (2006) using high resolution IKONOS data shows “the supervised classification on the unedited image identified water (pond) areas very well but had difficulty identifying emergent and forested/shrub wetlands. Upland areas were often confused and mixed with the emergent and forested/shrub wetlands.” (Fuller, Morgan, and Aichele, 2006) Similarly, Townsend and

Walsh (2001) showed the lowest accuracy for Sweetgum and (Wet) Oak-Maple-Sweetgum. They report “the Sweetgum class is highly variable in composition and often bears close resemblance to several other classes.” (Townsend and Walsh, 2001)

With the advent of hyperspectral scanners, large data arrays of spectral signatures are collected within very narrow bandwidths as most hyperspectral systems have the capability of utilizing several hundred different spectral bands:

Unlike multispectral imagery, which consists of disjointed spectral bands, hyperspectral imagery contains a larger number of images from contiguous regions of the spectrum. This increased sampling in spectrum provides a significant increase in image resolution—and thus in information about the objects being viewed. (Artigas and Yang, 2004)

Laboratory-derived spectral signatures are available for use to assist the sensor in classification. The resultant analysis has greater accuracy than conventional systems, and makes it “...possible to map plant species in coastal wetlands and relate their configuration and spatial arrangement to hydrological conditions influencing habitat heterogeneity -- and ultimately, biodiversity.” (Artigas and Yang, 2004)

Hyperspectral imagery similarly is useful in studying small scale ecology and environmental displacement within urban settings as well. “There is clearly a need to undertake studies, in conjunction with wetland scientists and managers, to determine whether information that can lead to improved management of these inland wetland ecosystems can be extracted from hyperspectral remote-sensing data.” (Jollineau and Howarth, 2008) Hyperspectral imaging supplies a greater number of narrowly spaced bands in which landscape data is sensed thereby ensuring the capability of better differentiating between very spectrally similar objects that may be adjacent to one

another. Intuitively, the resultant analysis should be far more accurate in classification of wetland features, even within sensors with only moderate spatial resolution.

The accuracy of hyperspectral imaging makes it possible to monitor and classify the characteristics of urban wetlands unlike many other systems. There are several possible classification algorithms available when processing imagery of any type. One of the most popular classification algorithms in remote sensing applications is the Maximum Likelihood method. However, certain algorithms have been developed to take full advantage of the spectral properties within hyperspectral datasets. The continuity of hyperspectral bands allows the possibility to apply very detailed mathematical methods, such as signature derivatives. Research by Sun et al. indicated that derivative processing will enhance relatively minute alterations, reduce sensitivity, and potentially remove background spectra from processed signatures. Multispectral systems lack this effective continuity, thus making such processing not relevant. Furthermore, results from Salem et al. determined that “conventional, statistically based methods used for multispectral data classification are not efficient when using hyperspectral data.”(Salem et al., 2005)

Much research has found great success with the use of the spectral angle mapper classifier (SAM) and matched filtered analysis (MF) with hyperspectral imagery. The MF technique “maximizes the response of the known endmember and suppresses the response of the composite unknown background; thus matching the known signature.” (ITT Visual Information Solutions, 2006) This approach rapidly detects features in the imagery with very similar spectral properties found in the spectral library’s associated feature. These similarities are based on the location of spectral curve peaks and valleys

between the pixel signatures and corresponding library signatures. This algorithm has the tendency to over-classify because slope of the spectral curve is not necessarily considered; only magnitude and the location along the electromagnetic spectrum. The SAM method analyzes spectral signatures with a little more detail and precision. “Treated as vectors in n-dimensional feature space, the SAM algorithm compares unknown pixel spectra to selected endmember spectra by calculating the spectral angle, in radians, between them.” (Jollineau and Howarth, 2008) They continue that, “minor spectral confusion between the shrub-dominated class and the other wetland plant communities, especially submerged aquatic vegetation.” (Jollineau and Howarth, 2008) SAM is not limited to hyperspectral data; any imagery acquired may be used as long as the dataset has undergone atmospheric correction to obtain surface reflectance as opposed to pixel digital numbers.

The most common hyperspectral scanners currently used in wetland research are mounted on low altitude aircrafts. Airborne Imaging Spectroradiometer for Applications (AISA) and Airborne Visible/Infrared Imaging Spectrometer (AVIRIS) are two very popular systems used in several different research applications. Due to the airborne platforms of these sensors, they achieve both high spectral resolution and spatial resolution. The main limitation to aerial hyperspectral platforms is that swath width and path length is drastically reduced when compared to satellite sensors, thus requiring several flight lines to cover the same extent covered by one satellite scan line. Despite this limitation, there has been limited research depicting the advantages of satellite

platform hyperspectral scanners over conventional satellite scanners regarding wetland classification as opposed to aerial hyperspectral scanners.

High spectral and spatial resolution from low altitude aerial sensors would be ideal for classifying wetland features, especially when considering small or long narrow spatial characteristics. As previously mentioned, however, aerial imagery will require a large number of flight lines to cover a potential study area, which will be extremely costly. To reduce this cost while still obtaining reasonably high spatial resolution, data fusion may be performed on low resolution hyperspectral imagery with higher resolution panchromatic or multispectral imagery:

The main objectives of image fusion are to sharpen images, improve geometric corrections, enhance certain features that are not visible in either of the images, replace the defective data, complement the data sets for the improved classification, detect changes using multispectral data and, substitute the missing information in one of the images with the signals from another source image. (Pande, Tiwari, and Dobhal, 2009)

There are several different algorithms available to perform data fusion, all of which have been tested extensively to determine the output quality of the fused image. The main algorithms used for data fusion are Principal Component Transformation (PCT), Gram – Schmidt Transformation (GST), and Color Normalized Transformation (CN). Research by Darvishi, Kappas, and Erasmi (Darvishi et al., 2005) showed little variation in GST and PCT output statistics. They go on to report, “the results show that the fusion process in general preserves the image statistics well, considering the mean, standard deviation, mode, and median of the histograms taken from the raw data and the fused image

channels.” (Darvishi, et al., 2005) Similar results have been found in research by Waldhoff et al. (2008) and Pande et al. (2009)

The main consideration to make when reviewing any data fusion results is that errors could exist in output datasets; therefore, it is important to strive for low root mean square errors. This will help limit possible pixel artifacts, and color / spectral distortion. Another factor noted by Darvishi et al. (2005) is that while statistics between different fusion algorithm results have relatively high correlation, there was much less correlation between all fusion results and raw imagery spectra. This exemplifies the need to carefully review and possibly test many different fusion methods to ensure the best possible output is used for further analysis.

For further analysis, landscape metrics will be used to analyze the final characteristics of wetlands within the study site to make a determination on habitat heterogeneity or potential fragmentation. Two categories of landscape metrics are considered for this task. One consists of metrics that focus on the composition within the landscape rather than the spatial arrangement of the composition within the landscape. The other category will focus on how the data and classes are spatially arranged within the landscape. Proportion, dominance, and Shannon Evenness are very common metrics used to describe the amount of area covered by each class, number of classes that dominate the landscape, and describes how evenly spread the classes are respectively. Spatial configuration will look at metrics including but not limited to Mean Patch Size, Probability of Adjacency, and Contagion evaluating the average size of each patch (a grouping of one class type by 4 or 8 neighbor rules), the probability that one cell of patch

type will reside next to another cell of any patch type, and measurement of overall clumping within the landscape per class type. Applying these metrics, or rather, a series of different metrics and plotting them together will likely show the importance and correlation between various different metrics within a landscape. There are many different sources available for metric analysis, where spatial extent and grain will have direct impact on the behavior of these metrics.

Scale plays a tremendous role in analyzing the behavior of a landscape. The appropriate extent for a study site will be based upon the size, length, or area in which the feature itself tends to be. “It is known that the scale of such maps affects landscape patterns, and therefore it is expected that landscape metrics also depend on scale.” (Carrão and Caetano, 2002) Wetland features will have a wide variety of shapes and sizes that may be studied, where some of these habitats may be very long and narrow. The studies by Carrão and Caetano (2002) show that very few metrics, including contagion and fractal dimension appear to show very little dependence on scale variations. On the other hand, values for patch density shows very interesting results in how scale changes. Essentially, as the extent of the imagery chosen increases, patch density decreases (Figure 2).

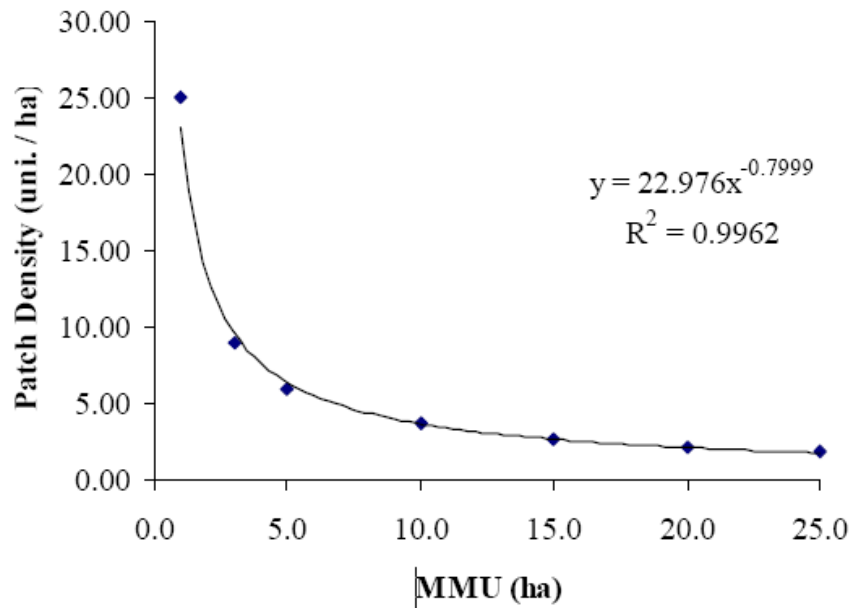


Figure 2. Relationship Between Patch Density and Scale (Carrão et al., 2002)

Artigas and Yang (2004) set to show how important scale is when interpreting landscape patterns based on landscape metrics. “The ramifications of scale are profound in studies in which habitat heterogeneity measurements are based on spatial metrics.” (Artigas and Yang, 2004) The studies they reported on with tide-open versus tide-restricted wetlands using landscape metrics tend to agree with the results from Carrão and Caetano.

Like scale, grain will directly affect the ability for an analyst to describe the heterogeneity of wetland habitats. With extent, the importance is to include enough area to cover the particular area of interest without including so much data that pattern analysis may be disrupted. Grain, however, focuses on the size of the cell in which data is captured. For very general results in landscape pattern analysis over large areas,

Landsat MSS data with 30 m cell resolution could be useful. However, this would only be possible if the features being studied cover a large area of at the very least 90 m². If the feature is smaller than this cell size, the dominant feature for that cell will take over in classification. This could likely result in misclassification of the wetland features, especially along the edges of feature types. Thanks to advances in modern technology, there are several sensors available with very fine cell resolution allowing for far more detailed analysis. “If landscape data continue to be available with increasingly fine resolutions suitable for design, management, and monitoring, understanding the effects of changing grain size on landscape pattern measurements will be critical to temporal analysis.”(Corry and Laforteza, 2007) Essentially, with increasingly fine resolution, sub meter pixel classification may someday be possible giving extremely accurate analysis with landscape metrics. Sidewalks that force fragmentation or connection within a nature reserve surrounding wetland habitats may be included within metrics analysis allowing even greater detail in how the habitat is behaving.

Inferences on environmental health or strength could be made based on landscape metrics within wetland habitats based on measures of dispersal and levels of dominance within the habitat. Wetlands affected by surrounding urban areas may have a greater likelihood for homogenous environments, where only the most aggressive or possibly invasive species will survive. Results by Artigas and Yang (2004) discuss that tide-open sites displayed healthier habitat with greater heterogeneity based a larger number of patch types and Shannon Diversity Index (SHDI) values. A graph of their results, showing

approximately 0.6 higher in tide open wetlands; therefore, since the points are not centralized near the point where $y = x$ there is not a similar distribution (Figure 3).

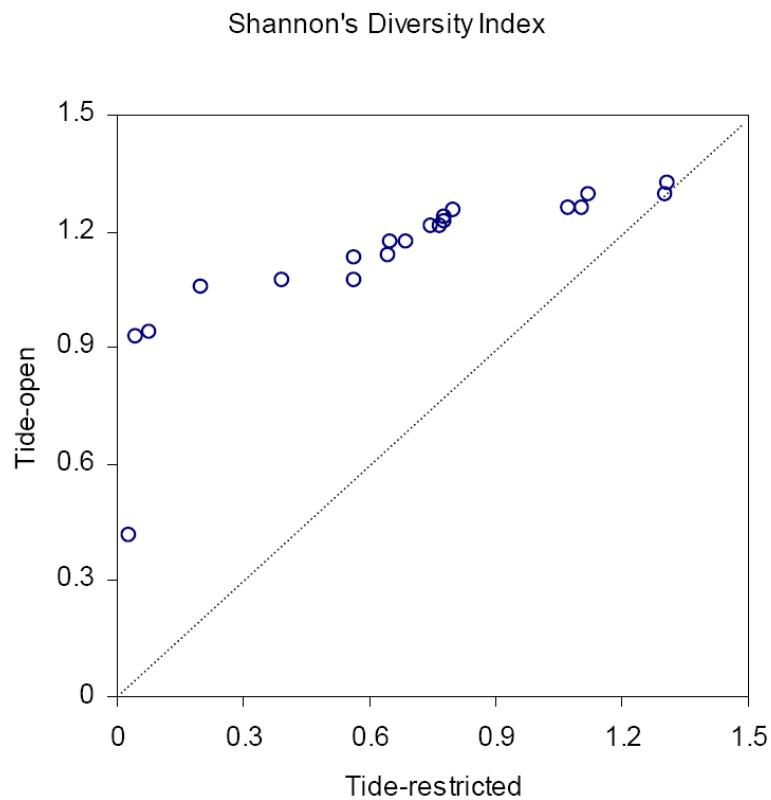


Figure 3. Shannon Diversity Results for Tide Open and Tide Restricted Wetlands (Artigas and Yang, 2004)

Research by Ehrenfeld within urban wetlands exemplifies this by showing that “species richness of both plant and animal groups may be higher than in comparable non-urban wetlands, due to the incursion of exotic and weedy species... and the removal of nutrient limitations due to pollutants in both air and water.” (Ehrenfeld, 2000) As species

richness increases, this would then show that dominance may have taken hold on the environment forcing the naturally heterogeneous habitat into a state of distress.

CHAPTER 3

STUDY SITE

North Western Jackson County, MO is a densely populated area with residential commercial, industrial, and agricultural areas dispersed along the Missouri River at its confluence with the Blue River (Figure 4) (Kansas City, MO National Land Cover Database, 2001). According to the United States Census Bureau 2007 Population Estimates, Jackson County has shown an increase in population of 12,010 people since 2000, and 37,624 since 1980. Many new homes and office spaces were required to accommodate such expansion, thus taking a toll on the natural landscape. There is a blend of emergent, freshwater, and riparian wetlands within this area, making it an ideal location for testing spectral variability in wetland mapping. Many wetlands run directly along edges of residential properties in this region, thus emphasizing the need to update classification, and manage these areas prior to further degradation. The project boundary for this study runs along a very mixed landscape with heavy population, commercial, and agricultural areas (Figure 5).

Updated wetland mapping is required to facilitate wetland protection or reconstruction in many of these areas. “To prevent further loss of wetlands, and conserve existing wetland ecosystems for biodiversity and ecosystem services and goods, it is important to inventory and monitor wetlands and their adjacent uplands.” (Ozesmi and Bauer, 2002) Such measures had been taken with the National Wetlands Inventory (NWI) from the late 1970’s to mid 1980’s. Kansas City, MO has undergone a variety of

landscape changes from then to the present day, making it necessary to update such datasets. It has been reported by the Missouri Department of Natural resources that the state has lost nearly 87 percent of its natural wetlands.

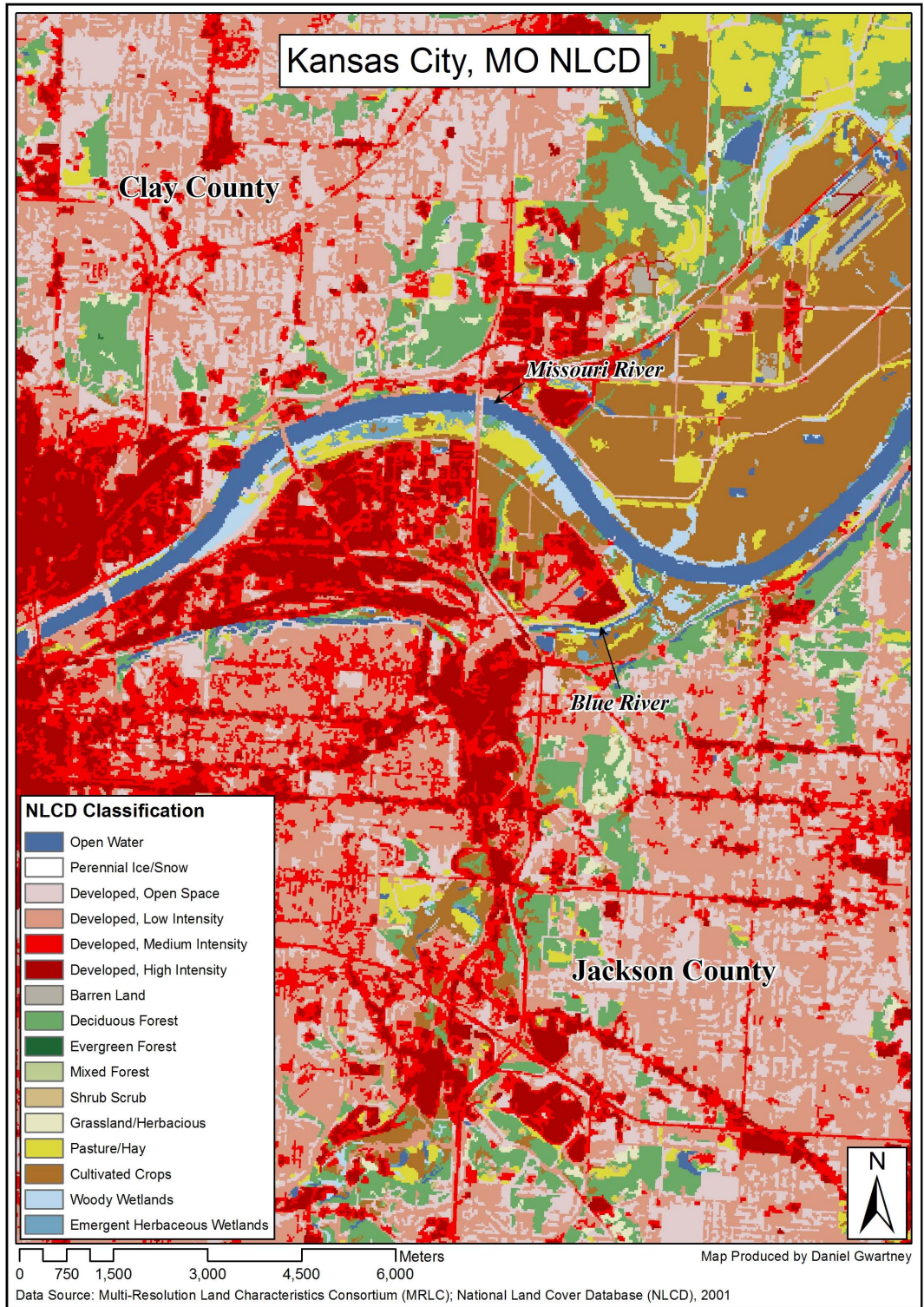


Figure 4. Kansas City, MO National Land Cover Database (NLCD) (2001)



Figure 5. Study Site Location

CHAPTER 4

METHODOLOGY

Earth Observing 1 / Hyperion Imagery Specifications

The Earth Observing 1 (EO-1) satellite was launched into orbit on November 21, 2000 as part of NASA's New Millennium Program; the extended mission of the satellite is currently under USGS supervision and continuation. The EO-1 orbit is designed to match that of Landsat 7 to collect imagery approximately one minute after Landsat 7 for direct comparison with the three imaging systems onboard. The temporal resolution for EO-1 is 16 days. The three sensors include ALI, Hyperion, and LEISA. ALI is a 10-band multispectral, push-broom style scanner, with one high resolution panchromatic band; panchromatic resolution is listed at 10m, while multispectral resolution is listed at 30m. The swath width is 37km and path length can be collected at 42 or 185km. LEISA is the first space-based test of an atmospheric corrector to help improve surface reflectance approximations at the sensor. Hyperion is a hyperspectral, push-broom style scanner, utilizing 242 spectral bands with a spatial resolution of 30 meters. The image swath width is 7.5km and path length can be collected at 42 or 185km. The spectral information onboard the Hyperion sensors range from 0.4 – 2.5 μ m. There are 35 visible bands, 35 near infrared bands, and 172 shortwave infrared bands. A narrow band spacing of 10nm, very detailed analysis is easily performed to extract spectrally similar features (ex. Plant species) as opposed to more generic or broad classes.

Initial dimensionality reduction should be performed by removing bands 1 – 7 and 58 – 76 because these are delivered as un-calibrated bands due to overlapping channels and large signal to noise ratios. Thus, the resulting dataset is reduced to a total of 196 useable bands for subsequent image processing (Figure 6). Level1 data is delivered as radiometrically corrected and geometrically resampled products. In general, atmospheric correction should be performed to take full advantage of the capabilities this sensor has to offer.



Figure 6. Raw Hyperion Imagery Subset

SPOT 5 Imagery Specifications

The SPOT 5 satellite was launched into orbit on May 3, 2002. SPOT 5 is a 4-band, push-broom style scanner, with one high resolution panchromatic band (Figure 7).

Bands 1 and 2 cover the green and red part of the visible spectrum, while bands 3 and 4 cover the near infrared and shortwave infrared parts of the electromagnetic spectrum respectively. The temporal resolution of SPOT 5 is two to three days pending latitude. Both swath width and path length are approximately 60km; therefore covering very large spatial area. SPOT 5 spatial and spectral resolutions are variable between each band (Table 3).

Table 3

SPOT 5 Spatial and Spectral Resolution

Band	Spatial Resolution	Spectral Region
Panchromatic	5m	0.480 - 0.710 μ m
Green	10m	0.500 - 0.590 μ m
Red	10m	0.610 - 0.680 μ m
Near IR	10m	0.780 - 0.890 μ m
Shortwave IR	20m	1.580 - 1.750 μ m

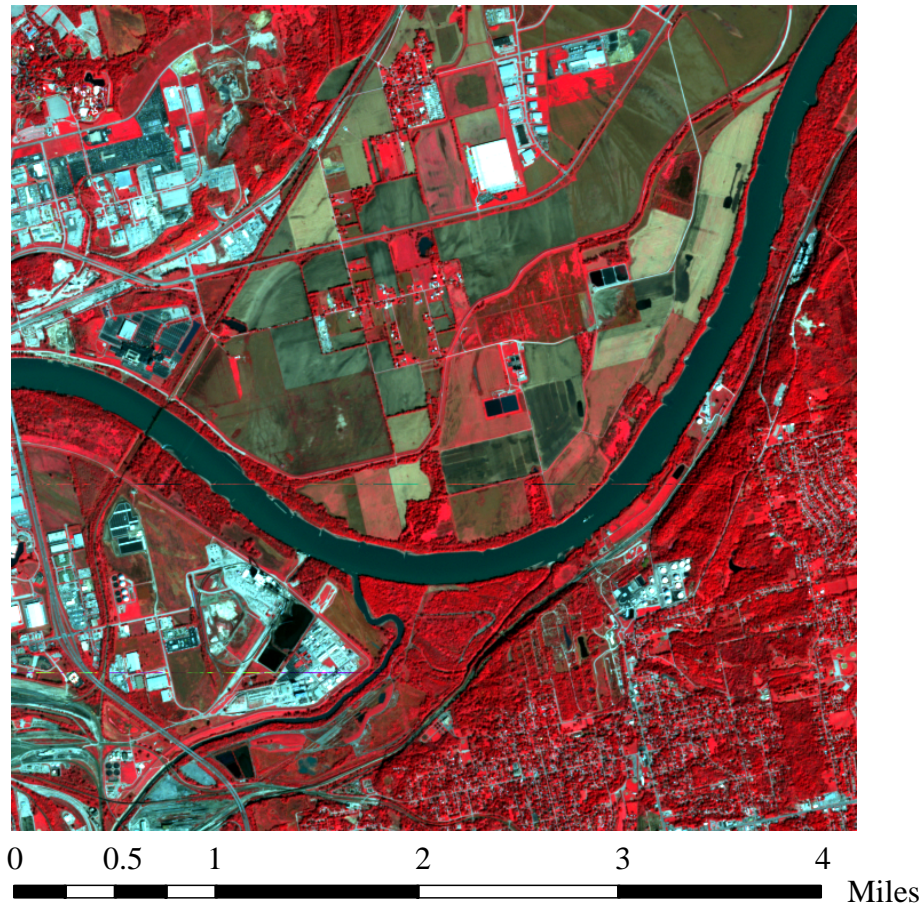


Figure 7. Raw SPOT 5 Imagery Subset

Atmospheric Correction

Level 1 data is generally delivered with pixels recorded as raw digital numbers (DN) representing the intensity of electromagnetic radiation for each spectral band. In order to obtain reflectance values, DN values must first be converted to radiance to display the energy units that each DN represents within a pixel in units of $W/(m^2 \cdot Sr \cdot \mu m)$. Hyperion DN values are converted to radiance by dividing visual near infrared bands 1 – 70 by a scale factor of 40 and the shortwave infrared bands 71 – 242

by a scale factor of 80. To obtain radiance for SPOT 5 imagery, an ENVI IDL module was executed to compute the following equation for radiometric calibration across all bands (Equation 1, ITT Visual Information Solutions, 2006).

Equation 1. SPOT 5 Calibration to Radiance

$$L = \frac{X}{A} + B$$

L = Radiance value in $W/(m^2 * Sr * \mu m)$

X = radiometric value per pixel from metadata

A = Sensor Physical Gain Value from metadata

B = Sensor Physical Bias Value from metadata

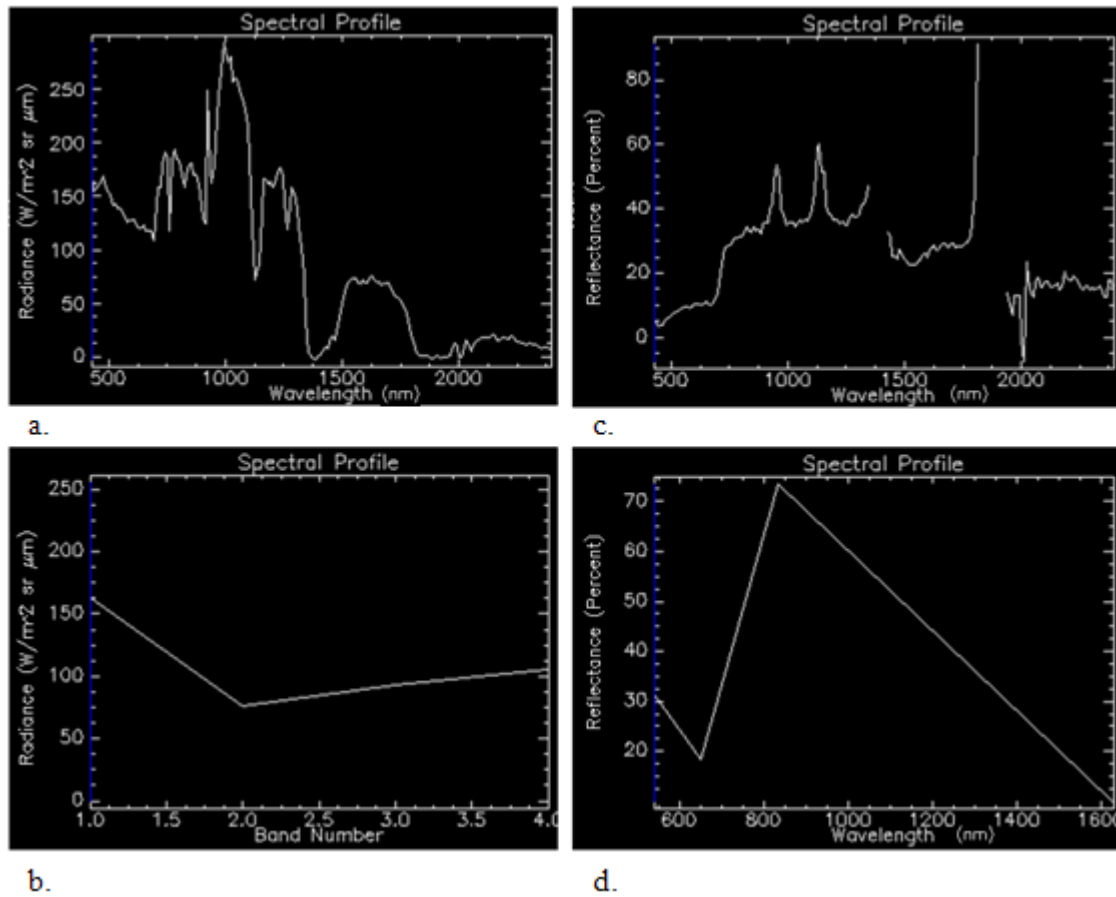
The module reads the sensor gain and offset information from the DIMAP metadata file for calibration.

Surface reflectance allows imagery to display typical spectral curves associated with specific materials. This enhances the subsequent classification algorithms ability to extract features of interest, as well as associate and mosaic operations for a multitude of imagery datasets. While this may be more useful for hyperspectral imagery due to detailed spectral information, such correction will readily enhance multispectral datasets by removing some haze and allowing certain advanced hyperspectral mapping techniques.

Fast Line-of-sight Atmospheric Analysis of Spectral Hypercubes (FLAASH), which utilizes the model, MODTRAN within the ENVI software package, was used to perform atmospheric correction for surface reflectance:

Using scattering and transmission properties of the atmosphere, the difference between the radiation leaving the earth and the radiation received at the sensor is modeled by radiative transfer codes having a typical atmosphere models for a large number of atmosphere types for calculation of atmospheric radiance spectrum on a pixel-by-pixel basis. The surface reflectance is attained by the ratio of radiance at the sensor to the model solar irradiance. (San, B.T. and M. L. Suzen, 2010)

Hyperion inputs to the model include sensor altitude (705km), collection date (2/2/2009), collection time (16:41:24), and center point latitude and longitude (39.112 and -94.489 respectively). Through consultation with NOAA and based on the collection temperature the atmospheric model utilized was U.S. Standard, the aerosol model was Urban, and the aerosol retrieval method was 2-Band (K-T). SPOT inputs to the model include a sensor altitude of 800km, collection date of 10/10/2008, collection time of 17:06:44, and center point latitude and longitude of 39.0404 and -94.6120 respectively. Through consultation with NOAA and based on the collection temperature the atmospheric model utilized was Sub-Arctic Summer, the aerosol model was Urban, and the aerosol retrieval method was 2-Band (K-T). Regarding both datasets, atmospheric correction was performed on non-geometrically corrected imagery to preserve image statistics by not introducing arbitrary zero cells that exist in geometrically corrected feature space. Figure 8 displays the difference between DN and reflectance profiles for both Hyperion and SPOT 5 imagery:



a. Hyperion vegetation DN profile; b. SPOT 5 vegetation DN profile; c. Hyperion vegetation reflectance profile (notice that atmospheric windows have been removed); d. SPOT 5 vegetation reflectance profile

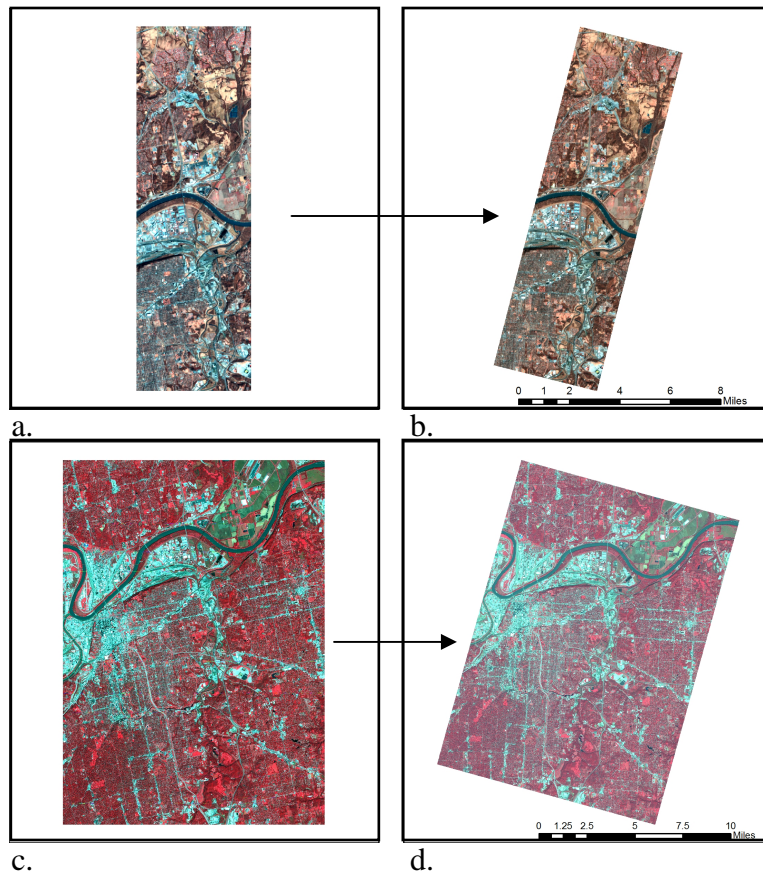
Figure 8. DN and Reflectance Profiles for Vegetation

Geometric Correction

Geometric correction was performed on atmospherically corrected datasets.

Individual ground control points (GCP) were selected from a previously registered SPOT 5 (2008) dataset for both Hyperion and SPOT 5 imagery datasets. Twenty five GCP's were randomly chosen, in a widely dispersed pattern for each dataset to ensure warped

results were not focused on a centralized location. Only permanent features such as road intersections, bridges, and large building corners were used to place the GCP's. Root Mean Square Error (RMSE) was calculated for these control points on both Hyperion and SPOT 5 to describe and validate image registration accuracy. The smaller the RMSE value, the closer the warped image is estimated to match the referenced image. A total RMSE of 0.57 was found for Hyperion, and an RMSE of 0.317 was found for SPOT 5; these values are less than 1, and deemed acceptable for image registration (Figure 9).



a. Un-Georeferenced Hyperion; b. Georeferenced Hyperion; c. Un-georeferenced SPOT 5; d. Georeferenced SPOT 5

Figure 9. Geometrically Corrected Hyperion and SPOT 5 Imagery

Hyperspectral Imagery Sharpening

In order to perform spectral sharpening techniques between the SPOT 5 and Hyperion datasets, both imagery was required to be geometrically corrected, and covering the same geographic space (Figures 10 and 11).

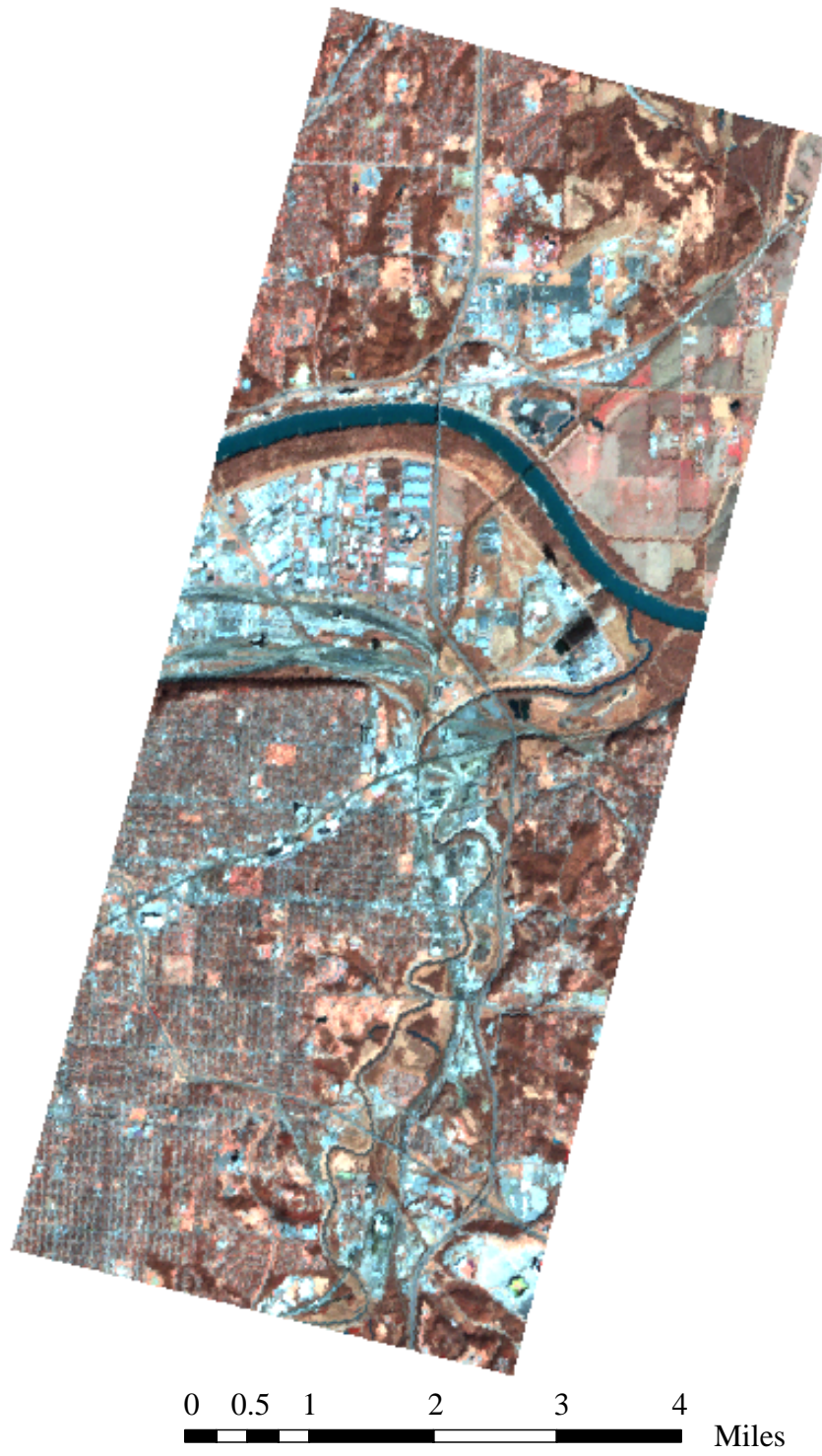


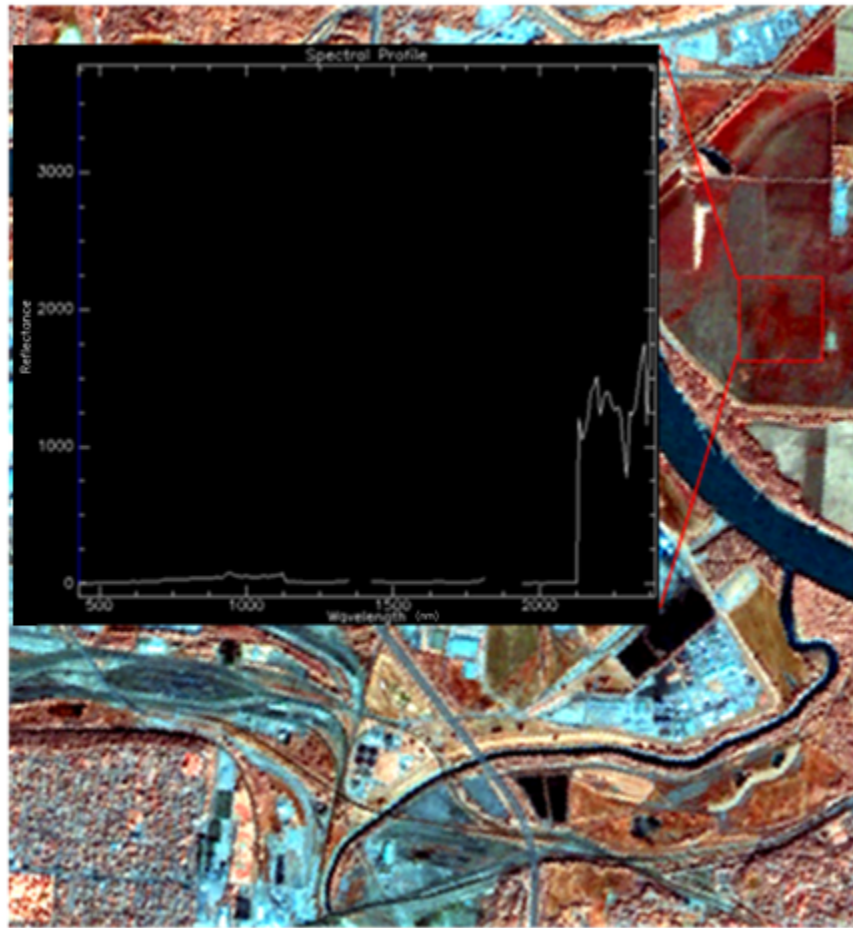
Figure 10. 30m Hyperion Imagery Study Area Subset



Figure 11. 10m SPOT 5 Imagery Study Area Subset

Color normalization (CN), principal components transformation (PCT), and Gram-Schmidt transformation (GST) spectral sharpening algorithms were performed with the Hyperion 30m datasets and the SPOT 5 10m bands; the panchromatic band with SPOT 5 was unavailable during processing.

Testing results displayed that CN produced very poor results in comparison to the other methods. While the appearance of the output dataset was very good, little correlation between resulting and original spectral profiles existed (Figure 12).



0 0.25 0.5 1
Miles

Figure 12. CN Sharpening Result with Spectral Profile

The profile associated with CN sharpening results indicates that a majority of the spectral information is lost during transformation. This methodology is not used for subsequent processing because of this.

Both GST and PCT algorithms produce very good sharpening results in both appearance and spectra. Output reflectance from both PST and GST results were nearly

identical, and showed very little difference from the raw Hyperion dataset. Simple statistics on bands 13 (Green), 23 (Red), and 44 (NIR) were computed for the raw, PCT, and GST datasets to determine the best resulting dataset for classification (Figure 13).

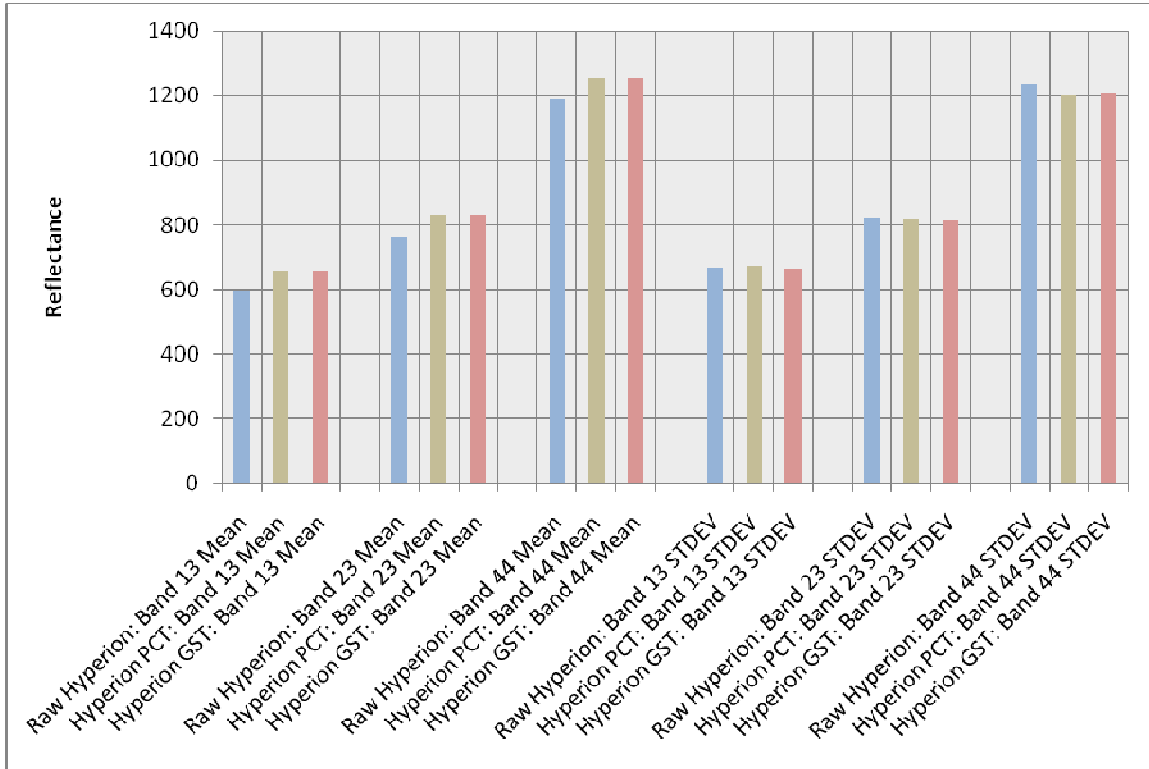


Figure 13. Raw, PCT, and GST Imagery Statistics

Based on the comparison of simple statistics between each dataset, both PCT and GST show very high correlation, and little difference from the raw dataset. The main differences are found in the standard deviations for bands 13 and 23, where the PCT algorithm sits slightly closer to the raw dataset value. The PCT fused result was chosen to proceed based on these two values and slightly better image appearance (Figure 14).

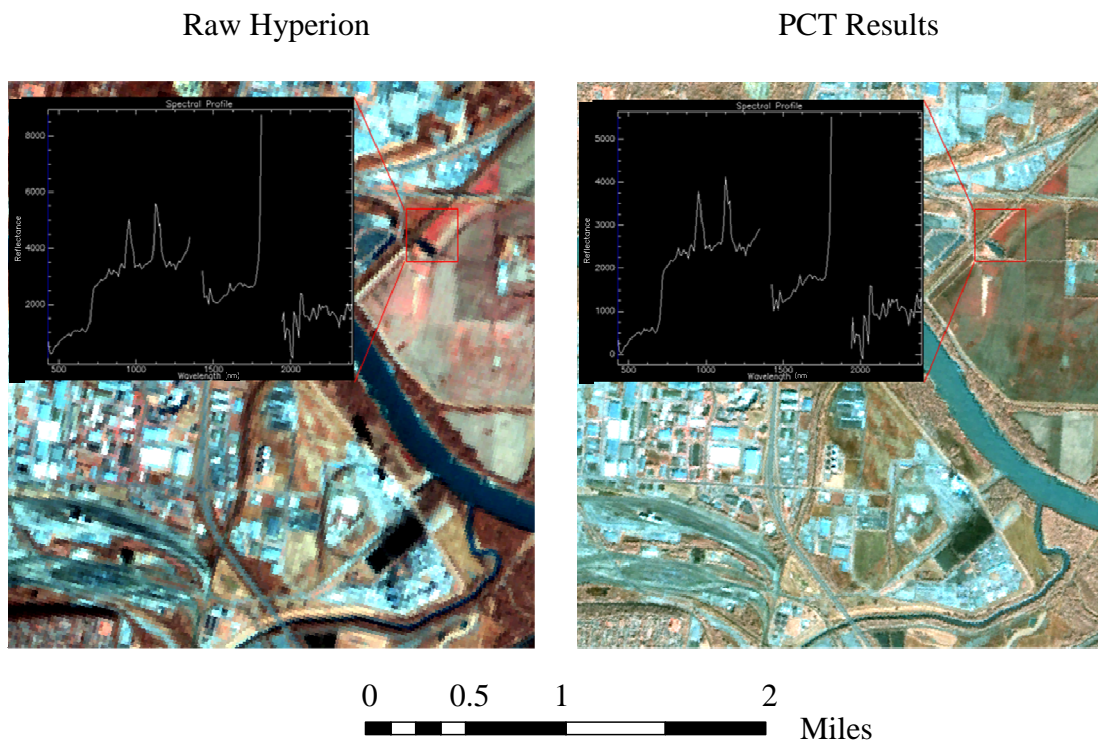


Figure 14. Raw Hyperion and PCT Comparison

Hyperspectral Derivative Processing

The limited spectral resolution available with multispectral imagery inherently displays spectral information through a series of disjointed spectral bands, forcing generalized spectral profiles for given features within the imagery. Comparatively, hyperspectral imagery offers the spectral resolution that produces relatively continuous spectral profiles. The benefit of these detailed profiles is not limited to simply locating parts of the electromagnetic spectrum that best detects specific features, but also allows advanced imagery analysis that is unavailable with multispectral datasets. “In term of

continuity attribute, it becomes possible to apply many mathematical methods to analyze hyperspectral data, such as derivative method.”(Sun et al., 2008) Taking the first derivative of hyperspectral imagery extrapolates the slope from the reflectance profile, thus enhancing relatively subtle changes within a curve (Equation 2).

Equation 2. First Derivative (Sun et al., 2008)

$$FDR_{\lambda_i} = \frac{dR}{d\lambda} = \frac{R_{\lambda_{j+1}} - R_{\lambda_j}}{\Delta\lambda}$$

FDR_{λ_i} = First derivative result

R_{λ_j} = Reflectance of band j, j+1, j+2;

$\Delta\lambda$ = Wavelength difference between bands j and j+1;

Similar to the SPOT 5 radiance calculation, the first derivative equation was used within an ENVI IDL module. This module was used on both the Hyperion 30m reflectance data (Figure 15), and sharpened reflectance data (Figure 16). Derivative profiles are nearly identical in shape, displaying even further success with imagery sharpening methodology. Subsequent image processing used radiance profiles in both imagery and spectral libraries, though reflectance profiles were still used for spectral range detection, feature separation, and class determination.

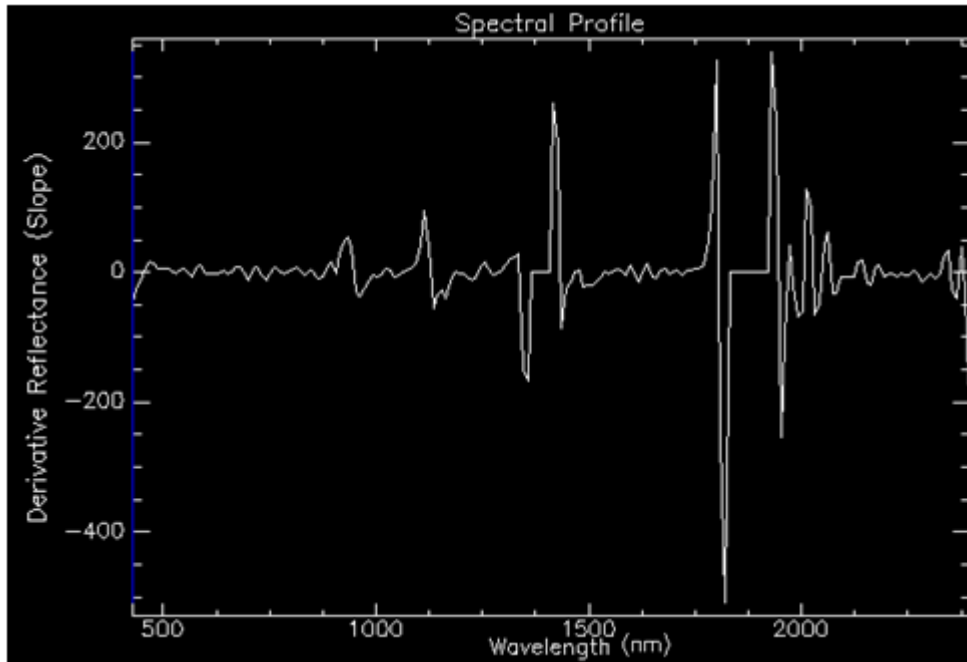


Figure 15. 30m Hyperion Derivative Profile

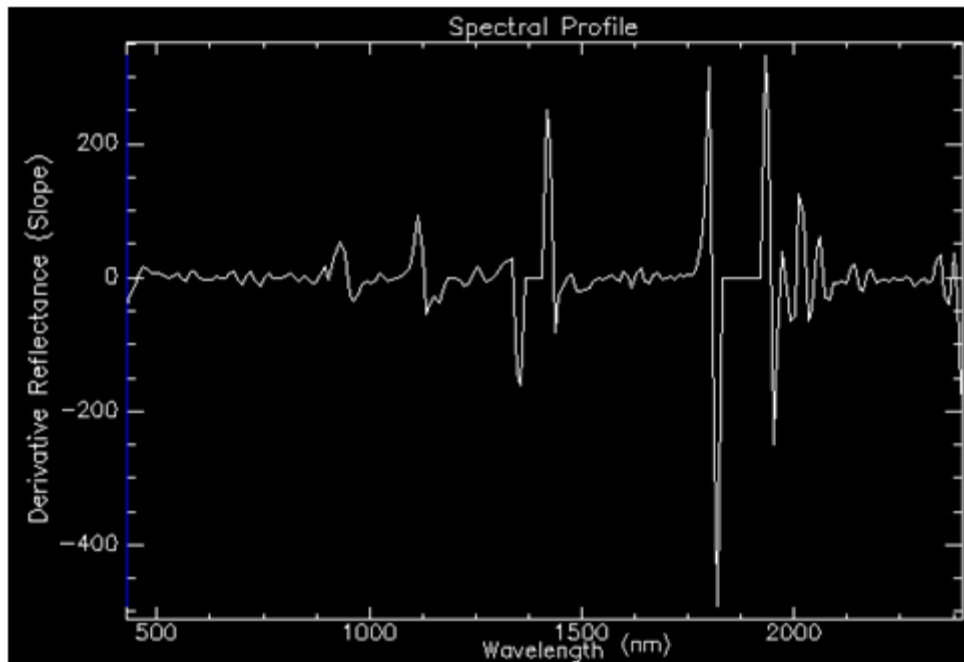


Figure 16. PCT Fused Derivative Profile

Signature Extraction

There are several sources of spectral libraries freely available to the public for a variety of landscape features. Previous spectral libraries may have little relevance to current imagery for many reasons, including seasonal variance, atmospheric conditions, and landscape patterns. Methodology to obtain current spectral information for any given target may be as labor intensive as performing field work with a hand-held radiometer, or simply generating spectral libraries from the imagery itself. In many cases radiometers will collect spectral information with 1nm band spacing, yielding very detailed spectral profiles spanning thousands of electromagnetic bands. The detailed signatures collected may be very useful in determining the best region of the electromagnetic spectrum to utilize for target detection. These signatures may also be applied towards feature extraction within the imagery itself. While this is very useful information, field work of this magnitude is a very costly endeavor in terms of both time and money.

Many practices will generate spectral libraries from the imagery itself to reduce the effort of field signature collection. These libraries will have less spectral information than a hand-held radiometer, but still cover several hundred bands of information; therefore, the in-scene spectral libraries will still be very detailed when compared to those of multispectral sensors. This methodology is not only efficient and less costly, but it will also produce target signatures representative of the spectral information found within the imagery itself. This is a very important consideration because reflectance values will be affected (ex. scattering) within the imagery due to radiation passing through the atmosphere, while libraries collected at ground level will have far less atmospheric

interference. Atmospheric correction tasks retrieved apparent reflectance observed by the sensor, but does not remove all affects the atmosphere has on incoming and outgoing solar radiation.

To build an in-scene spectral library, regions of interest (ROI) were developed as polygons for the atmospherically corrected Hyperion SPOT 5 datasets. ROI's were generated using source data from NWI datasets, NLCD datasets, limited site visits for validation, prior knowledge of the area, and high resolution National Agriculture Inventory Program (NAIP) aerial photography. Wetland ROI classes were comprised of riverine, freshwater pond, lake, forested / shrub wetland, and freshwater emergent in accordance with the NWI classification scheme. Additional classes for forest / trees, vegetation, agriculture / grazing, and impervious were included to cover a broad land cover classification scheme. The endmember selection tool within ENVI was used to analyze all pixels contained within an ROI polygon, and extract the average imagery spectra from pixels that appear to have the least amount of target mixing. Essentially, this tool assumes pixels that appear to fully contain spectra for one class feature and little to no spectra from another class feature are pure, and the signature for those pixels are extracted. The average reflectance signature is then computed for each class respectively, and saved as a spectral library for both Hyperion (Figure 17) and SPOT 5 (Figure 18).

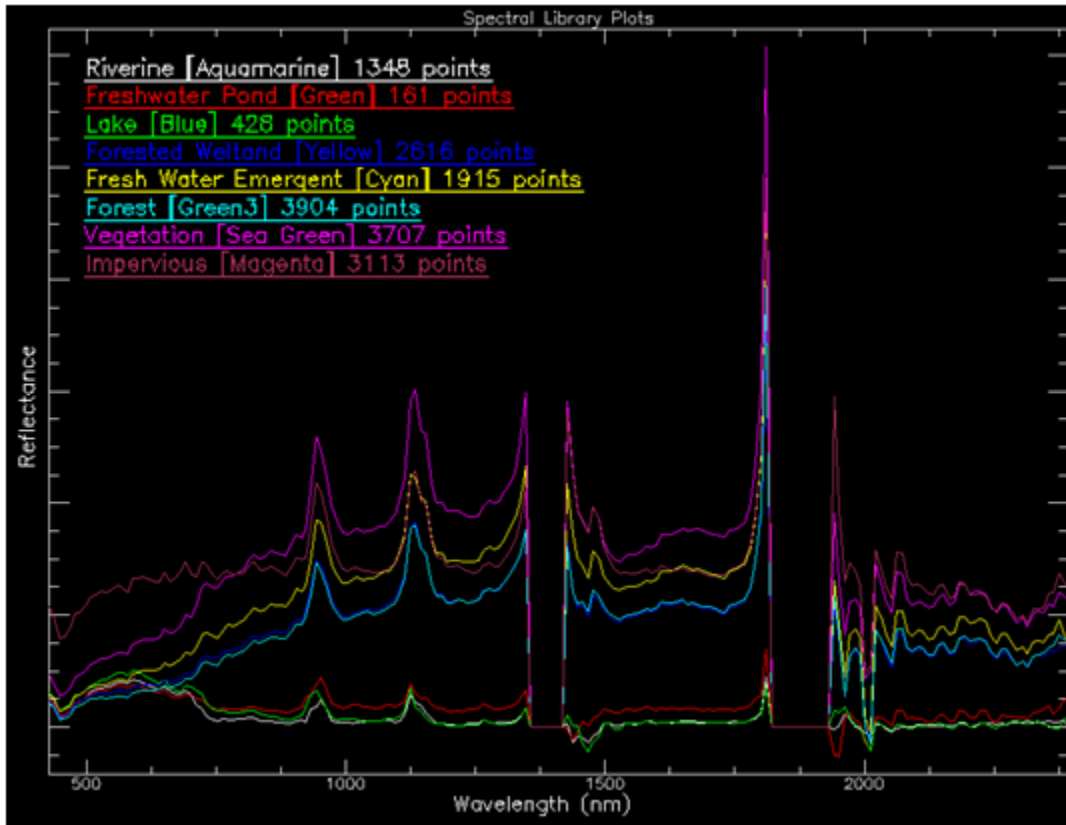


Figure 17. Hyperion Spectral Library Reflectance

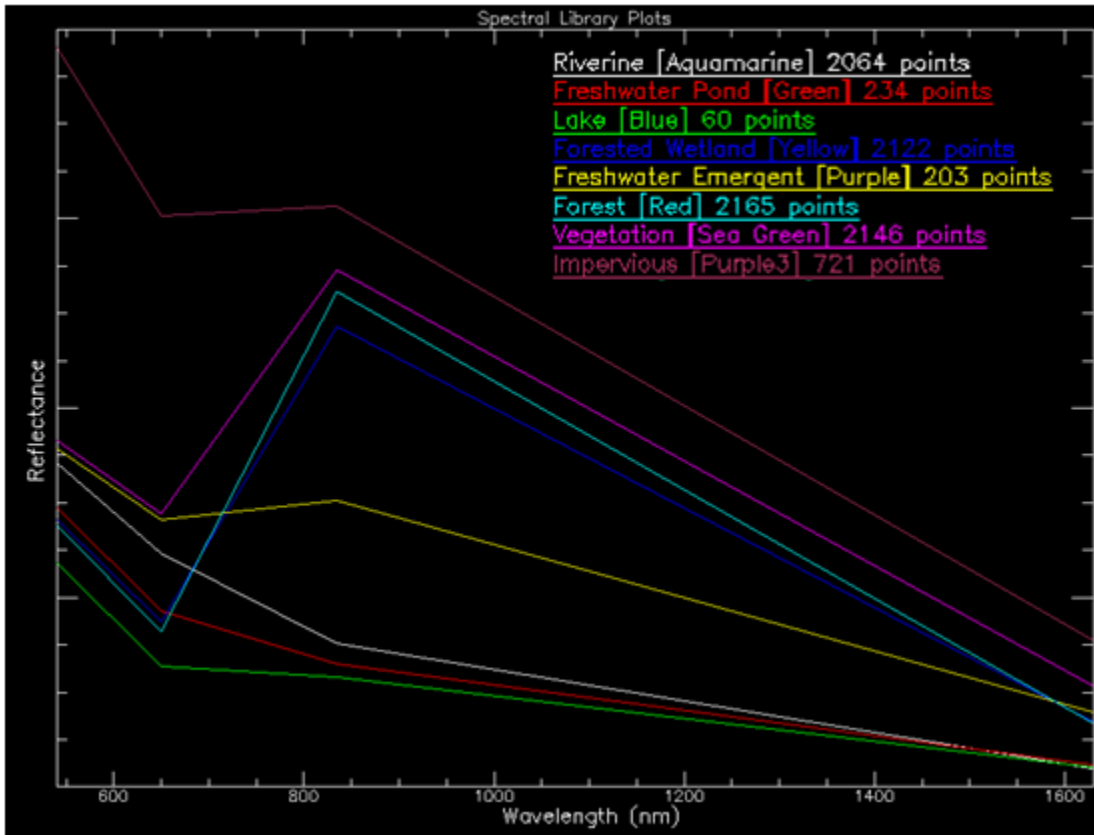


Figure 18. SPOT 5 Spectral Library Reflectance

As previously mentioned, derivative processing was performed on the atmospherically corrected Hyperion dataset. The same ROI's and endmember collection process for the Hyperion reflectance dataset were used to extract wetland and background spectra for classification and the derivative processed, raw imagery (Figure 19).

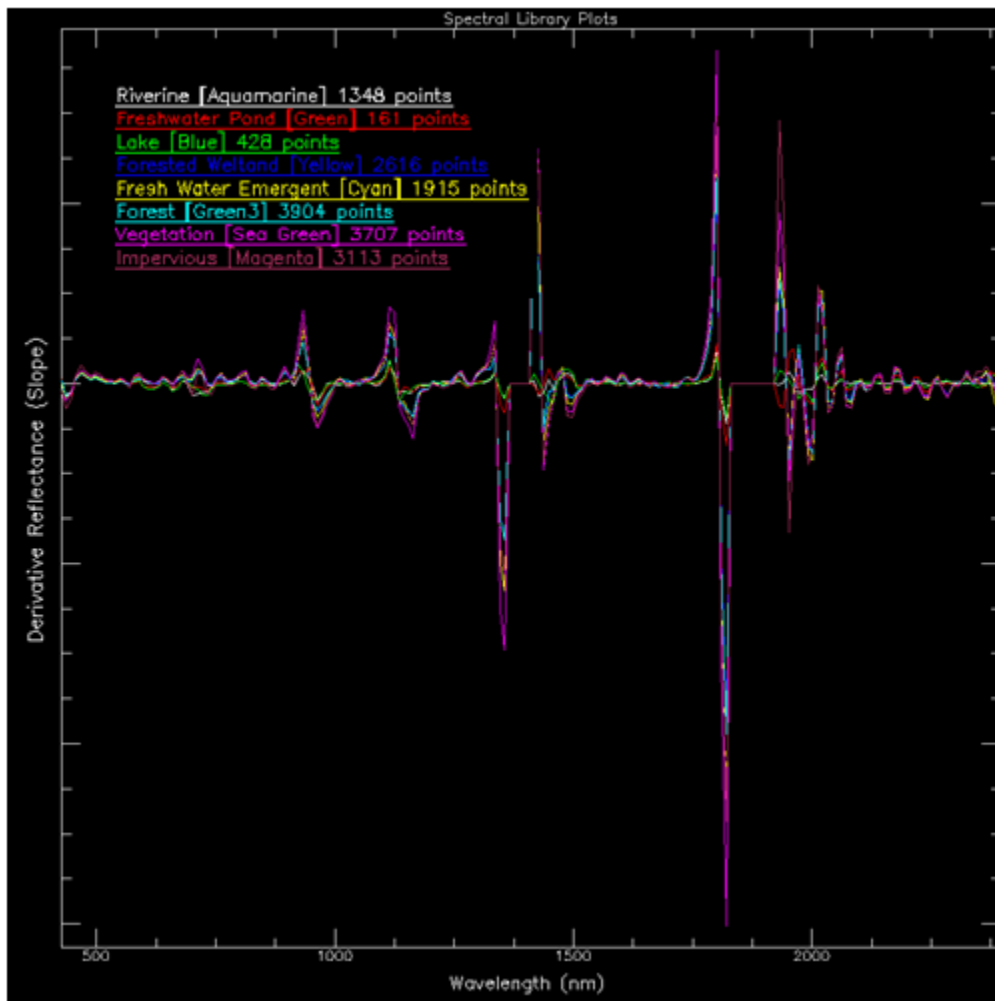


Figure 19. Raw Hyperion Derivative Spectral Library

Recalling the simple statistics gathered the output spectral profiles per pixel for PCT spectral sharpening performance, reflectance values per pixel have changed with the PCT fused dataset. Due to this, ROI's and endmember collections for this dataset were required. ROI's from the raw Hyperion dataset could not simply be used for the PCT sharpened dataset because the raw dataset covered a large area, and some ROI's fall

outside the spatial extent of the sharpened imagery. New ROI's were developed for the PCT fused dataset to extract a sharpened spectral library (Figure 20).

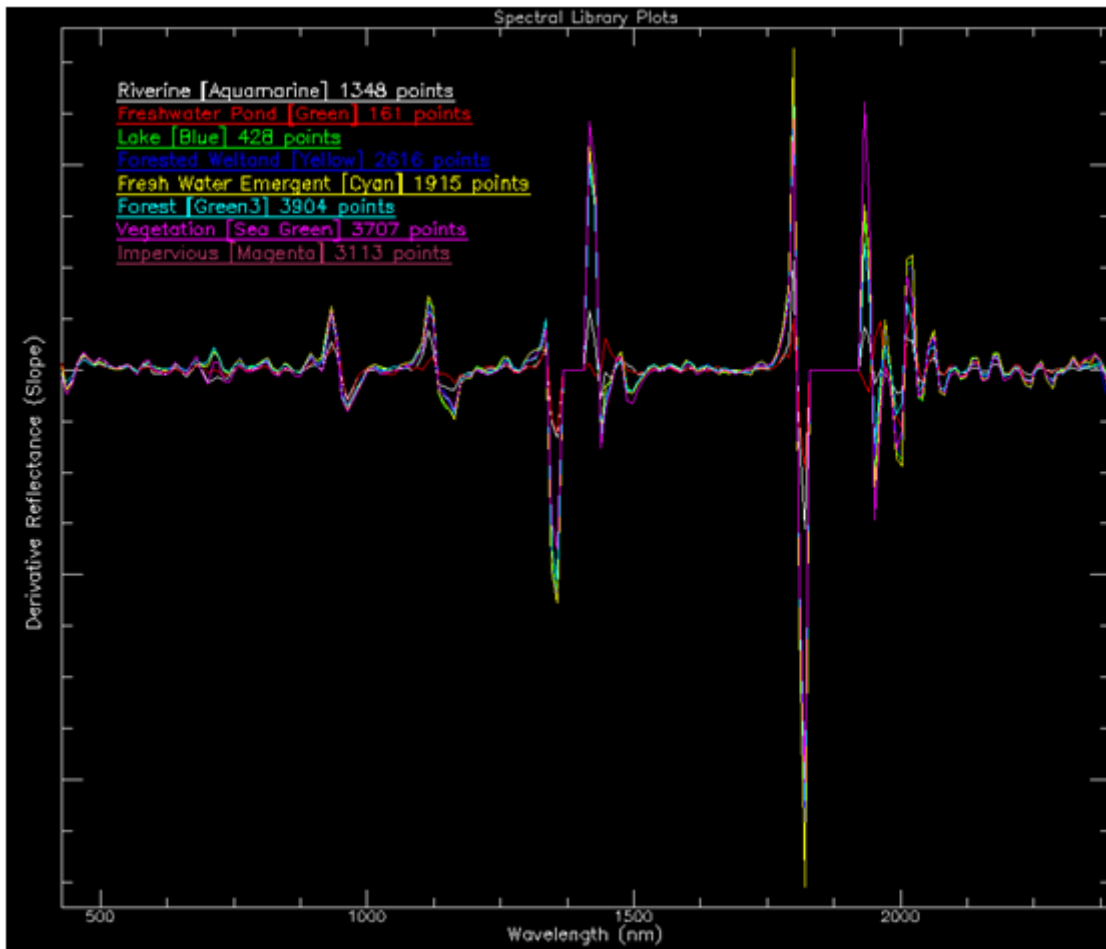


Figure 20. PCT Fused Spectral Library

The derivative class profiles for both raw and PCT fused libraries clearly show how similar the wetland classes are in terms of reflectance as opposed to simply using

reflectance profiles for classification. The subtle variations in slope key in more refined target detection for feature classification.

Hyperspectral Dimensionality Reduction

Dimensionality of hyperspectral datasets is very important to consider prior to classification. Initially, spectral bands for Hyperion have been reduced from 242 to 196 due to calibration issues inherent within the EO-1 Hyperion imaging system. It is still necessary to consider whether all the remaining bands contain pertinent information for subsequent image processing tasks. Not only will processing on a full set of hyperbands be computationally intensive, but certain parts of the electromagnetic spectrum could introduce misclassification with other features. Regarding wetland classification, consideration must be taken that all types of wetlands will likely respond in different parts of the electromagnetic spectrum similarly to other features within the landscape, including forests, agricultural lands, etc. It is possible, and necessary to review what specific region of the spectrum these features respond within that are even just slightly different from other features within the landscape.

There are several ways to check and reduce hyperband dimensionality. One of the more common methods to reduce dimensionality is Minimum Noise Fraction (MNF). MNF is essentially a two level principal components analysis (PCA) that is used to define eigenvectors within the dataset. The first level PCA is used to de-correlate and rescale noise statistics from the noise covariance matrix generated for each band. The resulting noise from the given bands will have no unit variance and no correlation between bands, otherwise known as noise whitening. The second PCA run transforms the noise whitened

data by rescaling the noise standard deviation and utilizing the original image. The final result of this transformation is a series of MNF statistics and eigenvalue plots.

Eigenvalues are defined as the change in magnitude of a mean vector that has no directional change under a given linear transformation (Strang, 2005). Initial dimensionality reduction was performed using the MNF process. MNF was run on the Hyperion dataset as an initial test for dimensionality reduction. Output eigenvectors indicated too many bands were needed to be removed. This indicated that MNF alone was not the best method for hyperband reduction.

The BandMax algorithm is a more recent approach to reduce hyperband dimensionality available in the ENVI software package. BandMax analyzes input target spectral profiles against all other input background spectral profiles available. The result from this algorithm is a subset list of bands that best detect the input target profile. After running this for all input targets, all significant bands are merged to one file in order to subset the hyperbands to only necessary bands for target classification. After running BandMax on the Hyperion reflectance data, the dimensionality was reduced by 90 bands leaving a total of 106 potential bands for processing. This helps reduce computational effort, while preserving a large amount of spectral information for detailed target detection.

Classification

The Normalized Difference Vegetation Index (NDVI) was initially run on all three imagery datasets (SPOT 5, Raw Hyperion, and PCT Fused) to assist in separating

healthy vegetation from non-vegetated areas within the imagery. NDVI is a commonly used and simple numerical remote sensing indicator for assessing the level of living vegetation from multispectral imagery datasets. NDVI is processed from the ratio of the difference between the near-infrared and red bands, and the sum of the near-infrared and red bands (Equation 3).

$$NDVI = \frac{NIR - RED}{NIR + RED}$$

Equation 3. Normalized Difference Vegetation Index

The rationale behind the functionality of this equation is that living green plants highly absorb incoming, visible, solar radiation (Blue, Green, and Red) for use during photosynthesis. The cellular structures of the leaves from living plants tend to reflect radiation in the near infrared part of the spectrum more readily as well. Non-vegetated features will tend to reflect poorly in the NIR wavelengths when compared to healthy vegetation. The higher reflectance of NIR wavelengths with healthy vegetation will yield resulting output values closer to 1. Soils tend to reflect in the red and somewhat higher in NIR wavelengths, but not as high as vegetation. Other non-vegetated areas such as impervious surfaces, water bodies, and clouds tend to be on the lower end of the positive values and into the negative values. Inspection of resulting NDVI files was performed to determine the appropriate thresholds for vegetation and non-vegetation extraction (Figure 21). NDVI output was then used as an analysis mask, thus reducing the probability of

misclassification by certain classes (ex. forested wetlands) from algorithms which may respond to large amplitude changes or trends as opposed to subtle features which are typical of vegetation signatures. For example, by using the results from the NDVI threshold to mask out non-vegetation pixels, the possibility to misclassify forest pixels over impervious features is effectively reduced.



Figure 21. SPOT 5 NDVI Vegetation / Non-Vegetation Threshold

The hyperspectral and multispectral methodology used for wetland and landscape classification employed two separate algorithms commonly used in hyperspectral image analysis. This methodology was used for raw Hyperion, PCT Fused, and SPOT 5 datasets. With both algorithms, each target feature was classified independently. The Matched Filter (MF) algorithm was first run on each individual landscape class. This approach rapidly detects features in the imagery with very similar spectral properties found in the spectral library's associated feature. These similarities are based on the location of spectral curve peaks and valleys between the pixel signatures and corresponding library signatures. The higher the MF response, the closer the algorithm matches pixel spectra to reference spectra. This algorithm has the tendency to over-classify because slope of the spectral curve is not necessarily considered; only peak magnitudes and their location along the electromagnetic spectrum.

The Spectral Angle Mapper (SAM) algorithm was run after all MF classifications were complete. SAM is a fairly more complex classifier than the MF algorithm in that it considers both the occurrence of spectral profile peak magnitudes, but also the slope of these curves as well. This is performed by converting the reflectance values to vectors and calculating the vector angle between pixel spectra and reference endmember library spectra (Figure 22).

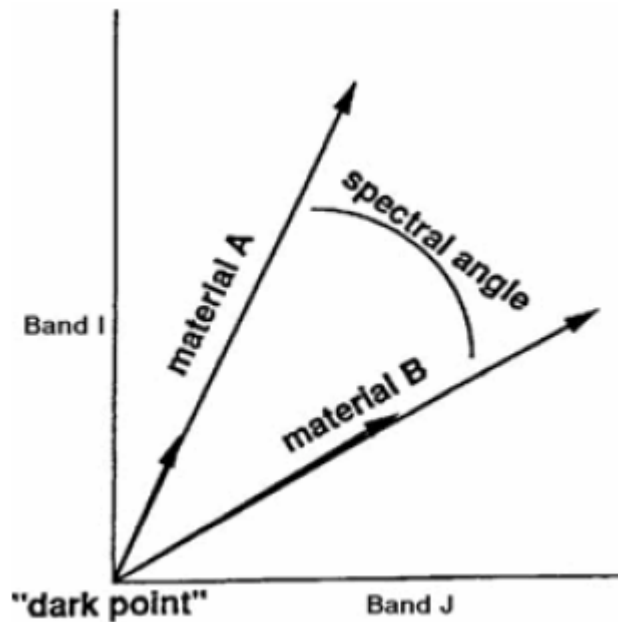


Figure 22. SAM Conceptual Reference (ITT Visual Information Solutions, 2006)

Smaller angles between pixel and reference spectra produce lower SAM response values. Different from MF outputs, SAM outputs with lower response values are considered good detections.

The final classification step used was using band math to perform the ratio of MF to SAM. This ratio “suppresses false positives that may be present in one” algorithm, “but not the other, while enhancing true positives.” (ITT Visual Information Solutions, 2006) For example, a pixel representing riverine features may have a high MF response, while the SAM response is very low. In this case, a high MF and low SAM response indicates this pixel will map as the riverine wetlands class. In this scenario, a high MF response value divided by a low SAM response value results in output response pixels

that are more likely to be good detections. Conversely, if there is a high MF response for a false positive detection on riverine wetland features, while the SAM response does not map the pixel as riverine wetland, the division between the two results suppresses the false response from the MF algorithm (Figure 23). To further reduce errors in classification, the NDVI product was used to mask out pixels that could introduce false positive classifications. Regarding riverine wetlands, for example, the healthy vegetation class extracted from the NDVI product was used to mask / remove pixels that were not identified as non-vegetated.



Figure 23. Raw Hyperion Riverine MF Divided by SAM Result

Histogram stretching, similar to that of the NDVI approach, was necessary to extract the appropriate pixels for the individual class ratio products. Threshold analysis began by reviewing the output ratio product histograms for the location along the normal curve where the slope is negative and beginning to level out near zero (Figure 24).

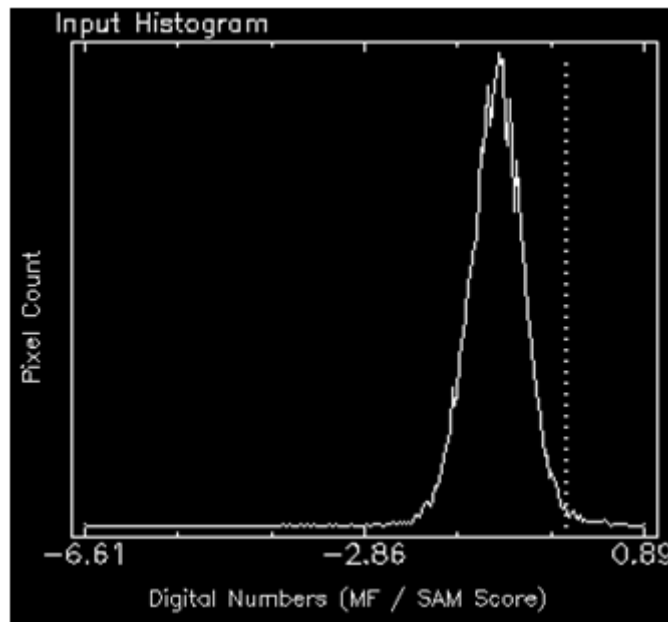


Figure 24. Raw Hyperion Riverine MF Divided by SAM Histogram

The further the threshold is set in the positive direction along the x-axis, the more confidence class representation is correct. However, this will also reduce the amount of pixels classified for this class, thus increasing the possibility for errors of omission. Conversely, the further the threshold is set towards the negative direction along the x-axis, the more pixels are included. Intuitively, this increases errors of commission from over classification. After sliding the threshold along the histogram to narrow in on

appropriate cutoff locations, the ratio pixels were rendered as standalone datasets for land cover dataset merging (Figure 25).

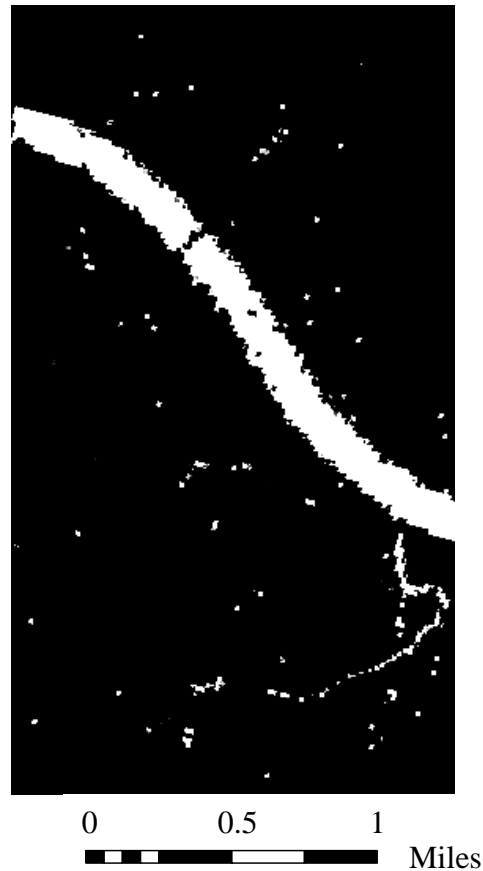


Figure 25. Raw Hyperion Riverine MF Divided by SAM Histogram Threshold Result

After thresholds were determined and rendered, post processing was performed to clean the individual files by the clump and sieve process in ENVI. Clumping was first performed to fill gaps between nearby pixels based on a 3 by 3 kernel. Any more or less than a 3 by 3 kernel filled far too many gaps or far too few gaps between pixels respectively. The sieve process was then performed to remove extraneous pixels that

give the output class datasets a salt and pepper appearance. Similar to clump, sieve utilizes a kernel pass to search through each pixel within the datasets. A 2 by 2 kernel was used while sieving to reduce only truly speckled classified pixels. Larger kernels would have reduced data that was unnecessary, and introduce further errors of omission. Finally, all individual wetland and background class datasets were merged into a single land cover dataset for each of the three imagery sources (Figure 26).

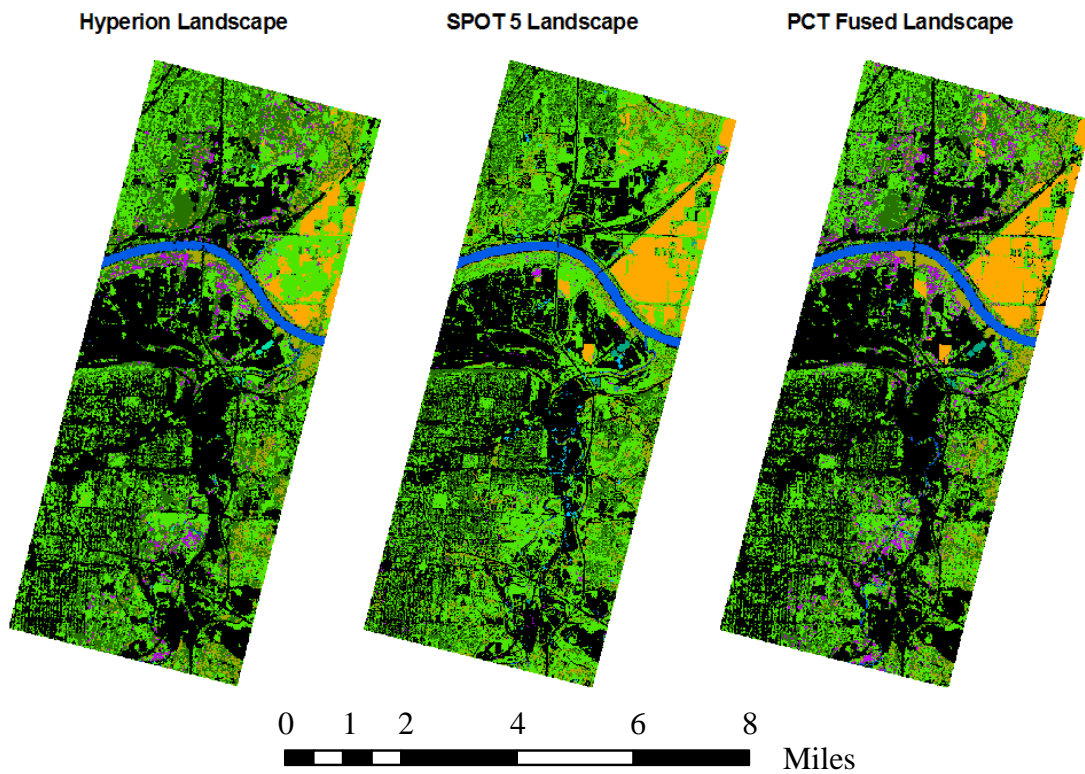


Figure 26. Hyperion, PCT Fused, and SPOT 5 Land Cover

Metrics

Patterns and processes within landscapes need to be quantified in order to fully understand how the landscape is behaving. The natural heterogeneity of a healthy wetland displays the importance of quantifying the pattern of such habitats. Modeling how these habitats change over time, or determining the difference in heterogeneity between urban and rural wetlands will directly display how the habitats are functioning differently. To do this, there is a multitude of statistical analysis techniques available, some of which may be found within different software packages. Furthermore, these statistics were also used to describe not only how detailed spectral information will improve classification results, but also how spatial resolution (grain size) directly impacts the results of landscape metrics. To assist in the execution of multivariate statistical analysis, a multivariate statistical software package developed by the University of Massachusetts Landscape Ecology Lab, entitled FRAGSTATS, was used to analyze classified results.

Prior to loading the classified results into FRAGSTATS, the classified Hyperion results were resampled to 10m resolution, so all three datasets have comparable pixel size. All classified imagery datasets were subset to the same boundary giving the same number of rows and columns for statistical analysis of 1787 and 1064 respectively. Regarding metrics calculations with FRAGSTATS, all NULL values were reclassified to 0 for each of the three classification output files. The result of these normalization steps

ensure that output metrics may be directly compared for landscape characteristics, as results from different imagery properties.

The search window used in FRAGSTATS may be set to either a four- or eight-neighbor patch rules. The four-neighbor rule simply reviews class values at each adjacent pixel to determine the number of patch types classified within the dataset; one on top, bottom, left, and right only. The eight-rule will also search diagonally adjacent cells to determine patch numbers within the dataset (Figure 27).

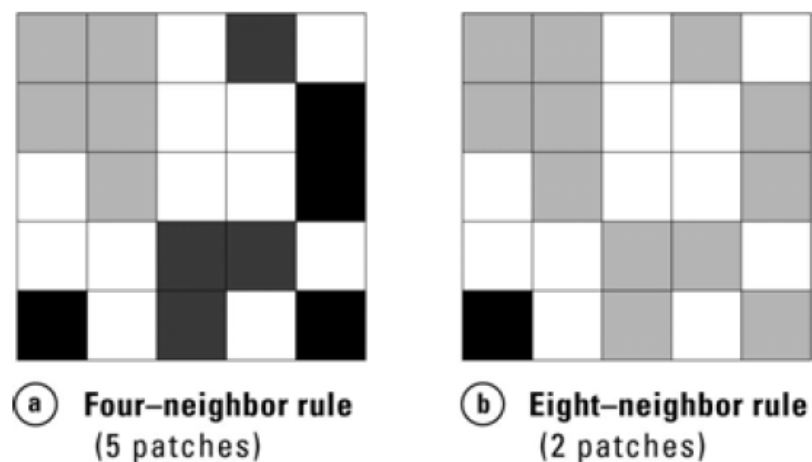


Figure 27. Four-neighbor and eight-neighbor Patch Differences (Turner et al., 2001)

FRAGSTATS is capable of running a tremendous amount of statistics on a landscape dataset. The three main scales for metric calculations are landscape, class, and patch. Patch metrics alone were not used in this analysis, however do play a role in class and landscape calculations. Class metrics are used to describe patterns and processes that exist within each specified class of the datasets, while landscape metrics tend to describe

the spatial relationship or dispersion of all classes across the entire area. Some redundancies exist between metrics at all scales, and others may have less importance given what the landscape research priority may be. Class and landscape metrics can be broken down even further to describe what patterns and processes the research is interested in. A set of Area/Density/Edge metrics were calculated for both class and landscape scales, while a set of diversity metrics were calculated for landscape scale only. FRAGSTATS outputs numerical values as indexes, percentages, or in units of hectares.

Class metrics used for analysis of Area/Density/Edge calculations included Total Class Area, Percentage of Landscape, Number of Patches, and Largest Patch Index. Class area describes landscape composition in terms of the quantity in which the landscape is comprised of a particular class per hectare. As class area approaches zero for a particular class, this class is more rarely found within the landscape (Equation 4).

$$CA = \sum_{j=1}^n a_{ij} \left(\frac{1}{10,000} \right)$$

CA = Class Area
 a_{ij} = area (m²) of patch ij

Equation 4. Total Class Area with units of Hectares (McGarigal, K. et al., 2002)

Percentage of Landscape was used to describe the proportion of which the landscape is comprised of a particular patch type in percent. The main limitation of this

calculation while using FRAGSTATS is that it considers all pixels within a classified dataset, including any background or pixels with no data associated with them. This was easily avoidable by ensuring classified datasets used for metrics had all cells with no data removed prior to processing. As percent of landscape approaches zero for a particular class, this class is considered rarer within the landscape (Equation 5)

$$PLAND = P_i = \frac{\sum_{j=1}^n a_{ij}}{A} (100)$$

PLAND = Percent of Landscape

P_i = proportion of the landscape occupied by patch type (class) i

a_{ij} = area (m^2) of patch ij

A = total landscape area (m^2)

Equation 5. Percent of Landscape (McGarigal, K. et al., 2002)

Landscape metrics used for analysis of Area/Density/Edge calculations included Total Area, Number of Patches, and Largest Patch Index. Total area is similar to class area calculations, but differs in that this calculation reports the total area extent of the landscape being studied rather than the area comprised of a certain class within the landscape. Alone, total area does not describe any importance on pattern or quantity of classes. The necessity of this calculation is that it was commonly used with subsequent metrics calculations (Equation 6).

$$TA = A\left(\frac{1}{10,000}\right)$$

A = total landscape area (m²)

Equation 6. Total Area with units of Hectares (McGarigal, K. et al., 2002)

Number of patches was used to provide a measure of fragmentation within class and landscape metrics. The main limitation to this metric is that it is often times not very usable by itself, and generally needs to be accompanied by a variety of other metrics to extract truly meaningful information. This was calculated for both class and landscape metrics, as they each provided slightly different information. The number of patches at the class scale represents the total number within a landscape per class, while at the landscape scale this is simply a total number of patches present regardless of class. Area calculations also allow the number of patches metric to provide the same information from other metrics including patch density and mean patch size regarding fragmentation of the landscape. Because the eight-neighbor rule was used while calculating metrics reduces the overall number of patches in the landscape (see Figure 27 for reference), providing a more realistic view on landscape fragmentation.

The largest patch index was used for both class and landscape metrics as well. This metric is reported the percentage cover of the largest patch found within each class (Equation 7) or within the full landscape (Equation 8) for the study area. The result from this percentage calculation measures a level of dominance for a given class within the

landscape. If the largest patch found has a relatively low percent coverage within the landscape, then the result indicates a low level of dominance because the largest patch size is relatively small in itself. This also indicates the possibility of a heterogeneous landscape.

$$LPI = \frac{\max(a_{ij})}{A} (100)$$

a_{ij} = area (m²) of patch ij
 A = total landscape area (m²)

Equation 7. Class Level Largest Patch Index Percent (McGarigal, K. et al., 2002)

$$LPI = \frac{\max(a_{ij})}{A}$$

a_{ij} = area (m²) of patch ij
 A = total landscape area (m²)

Equation 8. Landscape Level Largest Patch Index Percent (McGarigal, K. et al., 2002)

Additional metrics were used to describe the contagion and diversity of the classified images at the landscape scale. These metrics included Shannon's Diversity Index, Shannon's Evenness Index, and Contagion. Patch richness was not considered in this study because it is very similar to the number of patches metric in that it is reported

as a total number of patches. The main difference between patch richness and number of patches is that patch richness represents the number of patch types found within the classified landscape. At the landscape scale, the number of patches metric describes the total number of patches found regardless of class. The main limitation of patch richness is that does not describe the quantity of patch types, but rather provides a very simple approach to describe landscape composition.

Shannon’s Diversity Index (SHDI) is an approach at describing how diverse a landscape is with respect to the number of classes present. This may also be used as a way describe how evenly distributed landscape classes are amongst a landscape (Equation 9).

$$SHDI = -\sum_{i=1}^m (P_i * \ln P_i)$$

P_i = proportion of the landscape occupied by patch type (class) i
 m = number of patch types (classes) present in the landscape

Equation 9. Shannon’s Diversity Index (McGarigal, K. et al., 2002)

“SHDI equals minus the sum, across all patch types, of the proportional abundance of each patch type multiplied by that proportion.”(McGarigal, K., et al., 2002) The number of patches present in the landscape directly proportional to patch richness; as patch richness increases diversity increases. For example, if there is only one patch present in an entire landscape, $\ln P_i = 0$ giving SHDI the value of 0 and describing the environment

as homogeneous. The main limitation from SHDI is that the index value is limitless. This leaves room for debate on how a resulting index value is interpreted, i.e. how to determine what the high and low threshold is when describing distribution.

Shannon's Evenness Index (SHEI) is an approach at describing how evenly distributed all patch types are across a landscape, with respect to the number of classes present. SHEI has a limit of 1, which enables less arbitrary conclusion on the dominance of any patch type within the landscape. The equation for SHEI is very similar to that of SHDI; however, it is normalized by the number of patch types (Equation 10).

$$SHEI = \frac{-\sum_{i=1}^m (P_i * \ln P_i)}{\ln m}$$

P_i = proportion of the landscape occupied by patch type (class) i
 m = number of patch types (classes) present in the landscape

Equation 10. Shannon's Evenness Index (McGarigal, K. et al., 2002)

When the index result is closer to 1, this suggests maximum evenness within the landscape between patch types present. Conversely, lower results indicate that the landscape is heavily dominated by a patch type.

Contagion is a calculation that aims at describing how well like patches are dispersed throughout the landscape. Essentially, this calculation attempts to measure how aggregated, or clumped, the classes present within a landscape are with themselves. Contagion is affected primarily by dispersion and interspersions of patch types within a

landscape, and may therefore lead to inferences on fragmentation or habitat homogeneity (Equation 11).

$$CONTAG = 1 + \frac{\sum_{i=1}^m \sum_{k=1}^m \left[(P_i) \left(\frac{g_{ik}}{\sum_{k=1}^m g_{ik}} \right) * \ln P_i \left(\frac{g_{ik}}{\sum_{k=1}^m g_{ik}} \right) \right]}{2 \ln m} \quad (100)$$

P_i = proportion of the landscape occupied by patch type (class) i
 g_{ik} = number of adjacencies between pixels of patch types i and k
 m = number of patch types (classes) present in landscape

Equation 11. Contagion (McGarigal, K. et al., 2002)

Results from the contagion expression are multiplied by 100 to retrieve the percent level of aggregation within the landscape. When values are near 100, the index calculation indicates that the patch types are very well aggregated, leading to very few patch types existing within the landscape. Conversely, a contagion value close to 0 indicates the landscape is very disaggregated, and possibly suggests a very fragmented or nearly every pixel is representative of different patch types with few adjacencies.

CHAPTER 5

RESULTS

The spectral profile for the Hyperion, SPOT, and PCT fused data results were compared with each other to describe the overall outcome from the respective resulting land cover classifications. Classification totals and accuracy assessments were all performed for each dataset. Classification accuracy statistics, land cover totals, and visual quality were the criteria used to determine the overall success for each classification method performed in this study. Nine different land cover classes were used to build a generalized landscape for the study area, with a focus on wetland types and other generalized predominant landscape characteristics (impervious, forest / trees). As expected, the major sources of error reside in the Freshwater Emergent Wetland and Forested / Shrub Wetland classes between each other and various other landscape classes. In all three datasets, the Freshwater Emergent Wetland class had nearly the lowest user accuracy total; the SPOT 5 dataset had two classes with much lower user accuracy results, while this was the least accurate class for both Hyperion and PCT fused datasets. Overall, however, when considering the producer accuracy for the SPOT 5 Freshwater Emergent Wetland class, it is clear that this class is indeed the least accurate. Final analysis shows that the PCT fused dataset outperformed the results from the independent SPOT 5 and Hyperion datasets, and will be explained in greater detail within the following sections.

Hyperion Accuracy

The detailed spectral profiles developed from the Hyperion dataset allowed for very slight changes along the electromagnetic spectrum to be detected. The derivative processing capable with hyperspectral datasets allowed more detailed extraction of features, because of the output dataset's ability to exemplify regions along the spectrum where subtle slope changes exist; this was particularly useful for the SAM classification method. This is directly apparent in the misclassification between the Forest / Tree class and Forested / Shrub wetland class. For each class, 50 total randomly generated points were assigned to be verified for accuracy, giving a total of 450 points for the entire study site. The overall accuracy for the Hyperion landscape classification process was 85%. While this overall accuracy is generally low for a production result, this is still relatively good considering the amount of spectral overlap that tends to exist between most of these classes. Table 4 shows the individual class accuracies for the resultant classification, which also equates to the "User's Accuracy" for the dataset.

Table 4

Hyperion 30m Class Accuracy

Class	Classified (Correct)	Class Accuracy
Agriculture / Grazing	45	90%
Forest / Trees	43	86%
Forested / Shrub Wetland	40	80%
Freshwater Emergent Wetland	35	70%
Freshwater Pond	46	92%
Impervious	42	84%
Lake	44	88%
Riverine	47	94%
Vegetation	42	84%

The best performing classes based on user accuracy include Agriculture / Grazing, Freshwater Pond, Lake, Impervious, and Riverine classes. Though the Forest / Trees class was classified with an 86% user accuracy suggesting relatively good results, the producer accuracy only resulted with a 67% success. The Forest / Trees class had particular difficulty in separating Forested / Shrub Wetlands and Freshwater Emergent Wetlands; the two classes expected to cause most difficulty due to spectral overlap between adjacent classes. Commission errors of 14% are moderate, but unfortunately

omission errors of 33% are far too high when considering overall performance of the Forest / Trees classification. Forested / Shrub wetlands performed reasonably well with a producer accuracy of 87%, user accuracy of 80%, and omission / commission errors of 13% and 20% respectively. Table 5 lists all resulting accuracies and omission / commission errors associated with each individual class.

Table 5

Hyperion 30m Producer / User Accuracy

Class	Producer Accuracy	User Accuracy	Omission Error	Commission Error
Agriculture / Grazing	94%	90%	6%	10%
Forest / Trees	67%	86%	33%	14%
Forested / Shrub Wetland	87%	80%	13%	20%
Freshwater Emergent Wetland	80%	70%	20%	30%
Freshwater Pond	92%	92%	8%	8%
Impervious	82%	84%	18%	16%
Lake	100%	88%	0%	12%
Riverine	92%	94%	8%	6%
Vegetation	76%	84%	24%	16%

SPOT 5 Accuracy

Despite higher spatial resolution, the spectral profiles from the SPOT 5 multispectral dataset were greatly lacking in detail along the electromagnetic spectrum. This made it relatively difficult for the classification process to detect edges between spectrally similar features. This lack of detail in electromagnetic response also disallowed the ability to perform derivative processing for minor detections of slope change along the spectral profile. For each class, 50 total randomly generated points were assigned to be verified for accuracy, giving a total of 450 points for the entire study site. The overall accuracy for the SPOT 5 landscape classification process was 80%. Unlike the Hyperion dataset overall accuracy result, this is very low when considering future applications the dataset may be used for. However, classes with less spectral overlap or that are easily identifiable did perform better; thus, area and other statistical calculations may be more reliable for such classes as Riverine and Impervious. Table 6 shows the individual class accuracies for the resultant classification

Table 6

SPOT 5 10m Class Accuracy

Class	Classified (Correct)	Class Accuracy
Agriculture / Grazing	49	98%
Forest / Trees	43	86%
Forested / Shrub Wetland	37	74%
Freshwater Emergent Wetland	37	74%
Freshwater Pond	32	64%
Impervious	47	94%
Lake	24	48%
Riverine	48	96%
Vegetation	42	84%

The best performing classes based on the user accuracy include Agriculture / Grazing, Impervious, and Riverine. Much like the Hyperion dataset, the Forest / Trees class resulting in 86% user accuracy, but unfortunately the producer accuracy only resulted with a 74% success. Also consistent with the Hyperion results, the major source of confusion for the Forest / Trees class was within the Forested / Shrub Wetland and Freshwater Emergent Wetland. That being said, the Forested / Shrub Wetland class contributed far more to the inaccuracy of the class because of lacking spectral information that is not available within multispectral datasets. The least accurate classes

include Lake, and Freshwater Pond. These classes were commonly misclassified with additional water classes (either between themselves or with the Riverine class) and with the Impervious class. Very dark features such as asphalt parking lots or tar on rooftops have very similar reflectance, or lack thereof, with water features. This is caused by similar radiation absorption with these darker objects to that of water, unlike other pavement which reflects much more wavelength energy due to higher albedo rates. While the Impervious class had a very good user accuracy of 94%, the producer accuracy is very low. The over-classification of the Impervious class allowed for higher user accuracy results, while contributing very negatively by misclassifying pixels that belong to additional classes. Forested / Shrub Wetland and Freshwater Emergent Wetland errors of omission and commission were very similar to that found in the Hyperion landscape classification despite the lower producer and user accuracy total. Table 7 lists all resulting accuracies and omission / commission errors associated with each individual class.

Table 7

SPOT 5 10m Producer / User Accuracy

Class	Producer Accuracy	User Accuracy	Omission Error	Commission Error
Agriculture / Grazing	94%	98%	6%	2%
Forest / Trees	74%	86%	26%	14%
Forested / Shrub Wetland	90%	74%	10%	26%
Freshwater Emergent Wetland	86%	74%	14%	26%
Freshwater Pond	97%	64%	3%	36%
Impervious	48%	94%	52%	6%
Lake	92%	48%	8%	52%
Riverine	92%	96%	8%	4%
Vegetation	89%	84%	11%	16%

PCT Fused (Sharpened) Accuracy

Combining the higher spatial resolution of the SPOT 5 dataset with the higher spectral resolution of the Hyperion dataset provided the ability to spatially locate features with greater detail in feature boundaries, while spectrally separating features more readily along their feature space boundaries. It was not assumed that there would be a one to one relationship between pixels after fusion occurred, but rather, enhanced spatial and

spectral detail. Because there are far more pixels in the higher resolution data, it is known that the broad spectral information, in many cases, was interpolated to the higher spatial resolution pixels in the resultant dataset. Even with the understanding that this may not be considered a “purely” hyperspectral dataset, the overall performance of the classifications exceeded the accuracy results of the independent high spatial and spectral resolution datasets respectively.

For each class, 50 total randomly generated points were assigned to be verified for accuracy, giving a total of 450 points for the entire study site. The overall accuracy for the PCT fused landscape classification process was 88%. This accuracy total exemplifies the PCT fused datasets capability to take advantage of higher resolution pixels from one source coupled with greater spectral detail from another. While the overall accuracy is not as desirable as something in the low 90% range, this is still good considering the amount of spectral overlap that tends to exist between most of these classes.

Additionally, changes to post processing steps, minor refinement of threshold evaluation, or even slight changes to the spectral library could jump this to well within this range requiring far less effort than what is needed for the other two datasets. Table 8 shows the individual class accuracies for the resultant classification.

Table 8

PCT Fused (Sharpened) 10m Hyperspectral Class Accuracy

Class	Classified (Correct)	Class Accuracy
Agriculture / Grazing	47	94%
Forest / Trees	46	92%
Forested / Shrub Wetland	42	84%
Freshwater Emergent Wetland	39	78%
Freshwater Pond	41	82%
Impervious	49	98%
Lake	40	80%
Riverine	48	96%
Vegetation	46	92%

The best performing classes for the PCT fused dataset include Agriculture / Grazing, Impervious, Riverine, and Vegetation. It is notable that the Forest / Trees class improved tremendously from the other two datasets. Both the user and producer accuracies increased to be at 92% and 78% respectively. The Forested / Shrub Wetland class user accuracy increased as well to 84%. The producer accuracy for the Forested / Shrub Wetland increased from the Hyperion dataset, and decreased from the SPOT 5 dataset to 89%. These totals describe how the fusion process worked, and what contributions were made to the PCT fused dataset results. Ultimately, the higher spectral

resolution allowed the dataset to more readily extract forested / shrub features with higher water contents, while the spatial resolution from the SPOT 5 dataset helped to refine the class' spatial boundaries. However, the spectral overlap between the Forest / Trees and Forested / Shrub Wetland classes still existed, with Forest / Trees remaining as the primary source of confusion for the Forested / Shrub Wetland class.

The Impervious class suffered a bit in overall classification which may have occurred during the interpolation process when providing higher resolution pixels higher spectral resolution feature space. The Freshwater Emergent Wetland class remained the most problematic class, however, misclassifications were spread more evenly to other classes unlike the SPOT 5 dataset which had most misclassifications for the Tree / Shrub Wetland class within the Forested / Shrub Wetland class (similar to the Hyperion results). Table 9 lists all resulting accuracies and omission / commission errors associated with each individual class.

Table 9

PCT Fused 10m Hyperspectral Producer / User Accuracy

Class	Producer Accuracy	User Accuracy	Omission Error	Commission Error
Agriculture / Grazing	96%	94%	4%	6%
Forest / Trees	78%	92%	22%	8%
Forested / Shrub Wetland	89%	84%	11%	16%
Freshwater Emergent Wetland	83%	78%	17%	22%
Freshwater Pond	93%	82%	7%	18%
Impervious	84%	98%	16%	2%
Lake	100%	80%	0%	20%
Riverine	87%	96%	13%	4%
Vegetation	84%	92%	16%	8%

Metrics

Landscape and Class metrics were run to describe the overall “shape” of the study area land cover results. In an attempt to maintain consistency between datasets, the 30m Hyperion results were resampled to 10m spatial resolution. The overall class area for the Hyperion and SPOT 5 results were very comparable at 11,197.2 Ha and 11,197.0 Ha respectively. A slight difference between these two datasets and the PCT fused dataset

does exist, with the PCT fused overall class area reported as 11,191.5 Ha. This difference is a result of the slightly less than 1 to 1 relationship between the higher resolution SPOT 5 imagery and the lower resolution Hyperion imagery. Furthermore, each individual class area was analyzed between each dataset to describe distributions of the datasets (Table 10 and Figure 28).

Table 10

Class Area Distribution

Class	Hyperion Area (Ha)	Hyperion % Cover	SPOT 5 Area (Ha)	SPOT 5 % Cover	Fused Area (Ha)	Fused % Cover
Agriculture / Grazing	276.4	2.5%	567.9	5.1%	577.6	5.2%
Forest / Trees	2,332.9	20.8%	1,682.9	15.0%	1,772.1	15.8%
Forested / Shrub Wetland	481.6	4.3%	614.9	5.5%	458.0	4.1%
Freshwater Emergent Wetland	19.7	0.2%	44.0	0.4%	25.8	0.2%
Freshwater Pond	248.6	2.2%	39.5	0.4%	401.2	3.6%
Impervious	4,470.4	39.9%	4,167.7	37.2%	4,831.4	43.2%
Lake	1.5	0.0%	41.3	0.4%	2.6	0.0%
Riverine	206.5	1.8%	214.9	1.9%	234.1	2.1%
Vegetation	3,159.7	28.2%	3,823.9	34.2%	2,888.5	25.8%

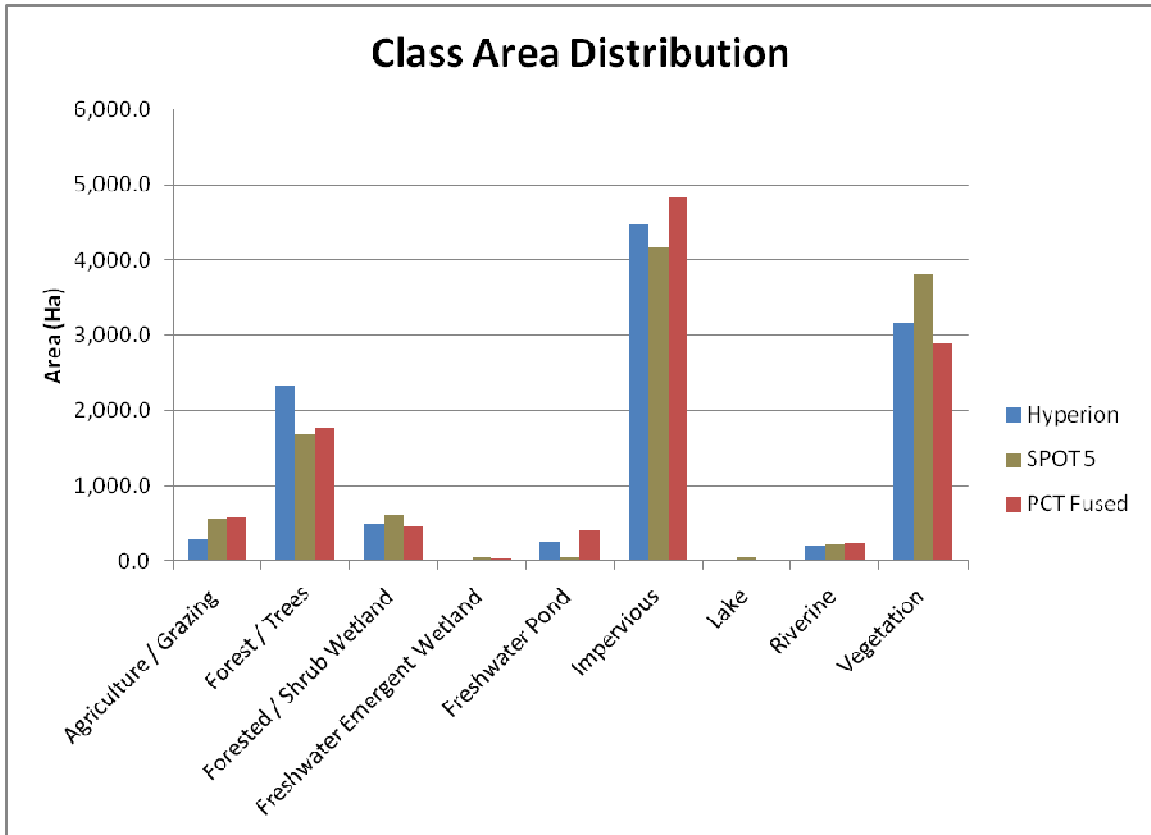


Figure 28. Class Area Distribution per Dataset

Individual class areas were reported for each dataset as well. The Hyperion, SPOT 5, and PCT fused classified results all showed that the predominant class in the study area is Impervious, which is as expected considering the urban nature of the study area. The Riverine class was comparable between the Hyperion, SPOT 5, and PCT fused datasets covering ~2% of each landscape. It is also clear that spatial resolution was the key element to successful classification of the Riverine Class. All three datasets had highly accurate results, but the 30m Hyperion dataset was unable to classify some of the narrower stream features running north and south in the study area. While the SPOT 5

dataset appears to have slightly cleaner edges along the Riverine class boundaries, the PCT fused dataset exceeded the SPOT 5 results due to having the advantage of both high spatial resolution and detailed spectral information (Figure 29).

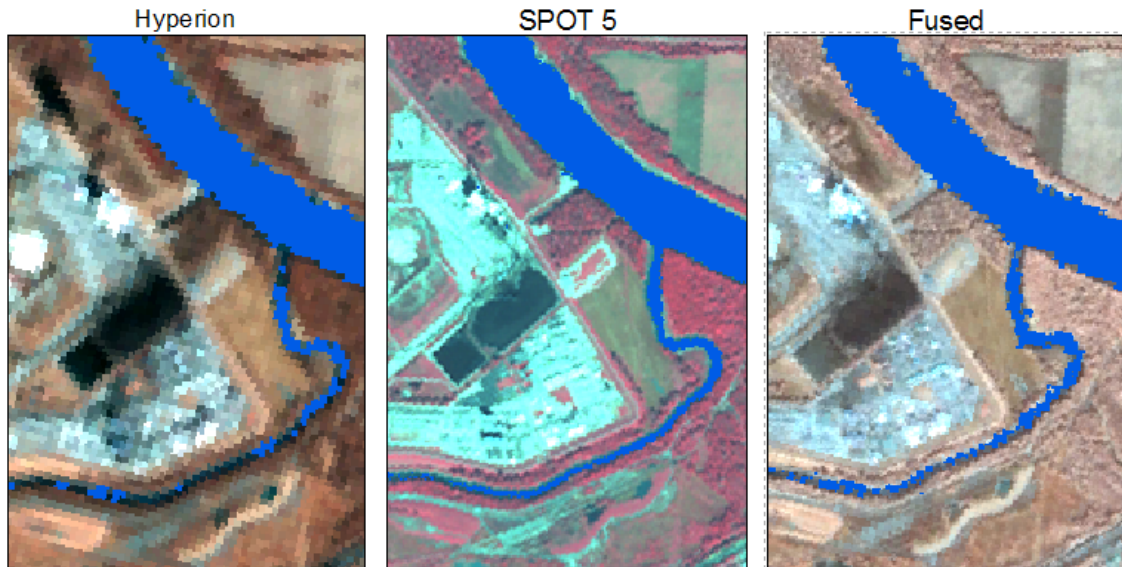


Figure 29. Riverine Classification Comparison

The Hyperion and PCT fused datasets are in agreement that “Lake” is the least dominant class in the study area, reporting 1.5 Ha and 2.6 Ha (0.0%) respectively, while over-classification within the SPOT 5 dataset reported lakes as comprising of 41.3 Ha and 0.4% landscape coverage. Similar results existed within the Freshwater Pond class as well. This suggests that enhanced spectral information within a dataset eased classification confusion between spectrally overlapping features such as dark pavement and certain water features.

Freshwater emergent wetlands were reported to cover 248.6 Ha and 2.2% landscape coverage for the Hyperion dataset, while 401.2 Ha and 3.6% landscape coverage was reported for the PCT fused dataset. The SPOT 5 dataset only classified 39.5 Ha and 0.4% landscape coverage for freshwater emergent wetlands. While the Hyperion and PCT fused results have relatively high levels of commission errors associated with them, these results are more likely to exist in the region due to low lying banks off major rivers as well as extensive floodplain within the region.

The Forest / Tree and Forested / Shrub Wetlands classes were major contributors to classification errors between each other, and with many other classes. The Forested / Shrub Wetland class was in agreement between the Hyperion and PCT fused datasets, with reports of 481.6 Ha (4.3% coverage) and 458 Ha (4.1%) respectively. The SPOT 5 dataset reported 614.9 Ha, or 5.5% landscape coverage and is accompanied by the highest error or commission between all three datasets. The Forest / Trees class for the Hyperion dataset shows far more coverage than the other datasets, with 2,332.9 Ha or 20.8%. The SPOT 5 and PCT fused datasets were much closer in agreement with reports of 1,682.9 Ha (15%) and 1,772.1 (15.8%) respectively. The PCT fused dataset accuracy for the Forest / Trees class far exceeds that of the other classes, especially regarding commission errors of only 8%. Ultimately, it is clear that spectral information helped differentiate the Forest / Trees class from other classes, while enhanced spatial information assisted with defining feature boundaries, thus reducing the commission error rate.

Measures for landscape heterogeneity were taken with the number of patches, patch density, and largest patch index calculations at the class and landscape metrics

scales. Landscape measurements show that the Hyperion dataset contained 70,066 patches, the SPOT 5 dataset contained 114,677 patches, and the PCT fused dataset contained 95,585 patches. The major difference between the SPOT 5 and the Hyperion datasets is due to differing resolutions and aggregation steps during post processing. The slightly less exaggerated change from the SPOT 5 and PCT fused datasets is a result of higher resolution coupled with detailed spectral information. The limited spectral detail in the SPOT 5 dataset found more patches due to spectral overlap between class types. Class boundaries were more easily classified with higher degree spectral data, limiting the number of segregated patches within the resultant datasets, while finding more patches than the 30m Hyperion dataset due to higher spatial resolution leading to more detailed / less aggregated results. Though the number of patches metric does not convey the most useful information by itself due to lack of information regarding patch sizes and spatial distribution, the results from these calculations tend to suggest that the landscapes for each dataset tends to be relatively heterogeneous, or moderately dispersed. The largest patch indexes were reported as 1.56, 1.40, and 1.54 for the Hyperion, SPOT 5, and PCT fused datasets respectively. Alone, these values do not tell us much. Class level metrics describe these statistics in a much clearer manner. Class level number of patches and largest patch index calculations were run to describe in greater detail how the landscape patterns exist within the study area (Table 11).

Table 11

Number of Patches and Largest Patch Index Distributions

Class	Hyperion Number of Patches	Hyperion Largest Patch Index	SPOT 5 Number of Patches	SPOT 5 Largest Patch Index	Fused Number of Patches	Fused Largest Patch Index
Agriculture / Grazing	1,515	0.12	1,921	0.66	1,394	0.66
Forest / Trees	20,996	0.52	38,043	0.03	29,668	0.38
Forested / Shrub Wetland	7,354	0.05	19,290	0.00	10,598	0.01
Freshwater Emergent Wetland	5,816	0.00	1,898	0.00	11,429	0.00
Freshwater Pond	287	0.00	1,454	0.00	405	0.00
Impervious	9,873	1.56	19,747	1.40	12,468	1.54
Lake	26	0.00	1,485	0.00	76	0.00
Riverine	713	0.15	1,229	0.15	1,256	0.15
Vegetation	23,486	0.60	29,610	1.00	28,291	0.24

At the class level, all three datasets showed that the Forest / Trees and Vegetation classes had the two highest numbers of patches. However, the Hyperion dataset indicates that there are more Forest / Trees patches in the landscape than there are Vegetation, which differs from the results in the SPOT 5 and PCT fused classified datasets. This

difference likely exists primarily due to spatial resolution differences; there should be little influence from errors of omission / commission since all three had very similar results from the accuracy assessment process. It is also noted that the Hyperion, Impervious class underestimated the number of patches when considering the results from the SPOT 5 and PCT fused datasets. Spatial resolution and lower accuracy directly impact the total number of segregated patches that exist for this class in the Hyperion dataset (Figure 30).



Figure 30. Impervious Classification Comparison

Essentially, it is clear in the number of patches metrics for all three datasets that the grain (spatial resolution) of the datasets impact the number of patches found in the datasets. Likewise, the SPOT 5 dataset showed far more patches for all classes than either the

Hyperion or PCT fused datasets except for the Lake and Freshwater Pond classes. These classes suffered from decreased spectral information to accurately separate different water types within the SPOT 5 classified landscape. The PCT fused dataset was benefited by higher resolution which increased the number of patches from what was found in the Hyperion classified landscape, and higher spectral resolution which decreased the number of patches found from what was found in the SPOT 5 classified landscape; thus, indicating that the PCT fused dataset gave a better perspective of the possible fragmentation within the landscape for this study area (Figure 31).

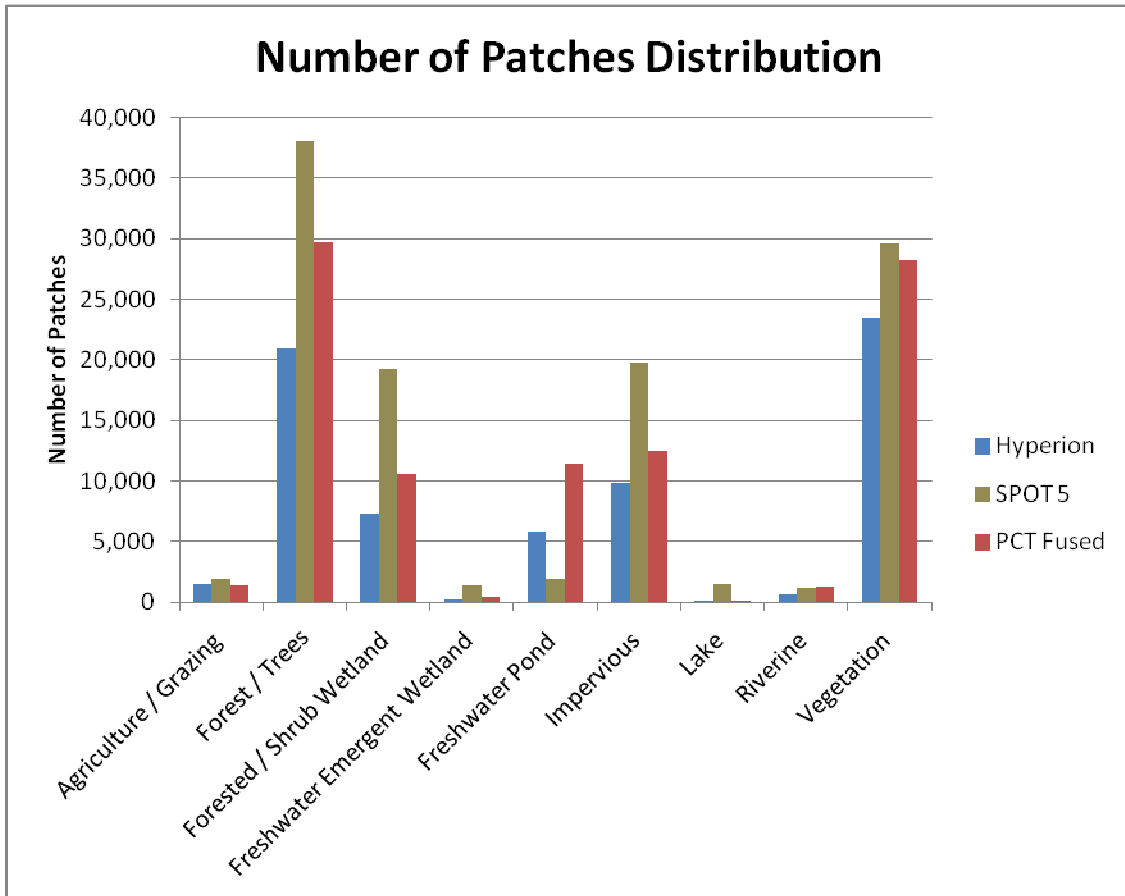


Figure 31. Number of Patches Distribution per Dataset

At the class level, the largest patch index was used to determine the most dominant class in the study area landscape. Unlike the number of patches metric, which inferred upon the notion that the Vegetation and Forest / Trees classes made up the majority of the landscape, the largest patch index defines which class appears to be the most dominant by considering the maximum area of each patch within a class. Essentially, if a class has more patches than any other class, but all the patches are relatively small, it is possible that this class is still not the most dominant. The largest

patch index found that the Impervious class was the most dominant class in the Hyperion, SPOT 5, and PCT fused datasets with values of 1.56, 1.40, and 1.54 respectively. The Vegetation and Forest / Trees classes still comprise of higher dominant land cover types in the landscape, but still not as prevalent as the Agriculture / Grazing areas in the northeastern portion of the study area. By normalizing the number of patches metric and reviewing against the largest patch index, fragmentation in the landscape may be better inferred upon within each class independently (Figures 32, 33, and 34).

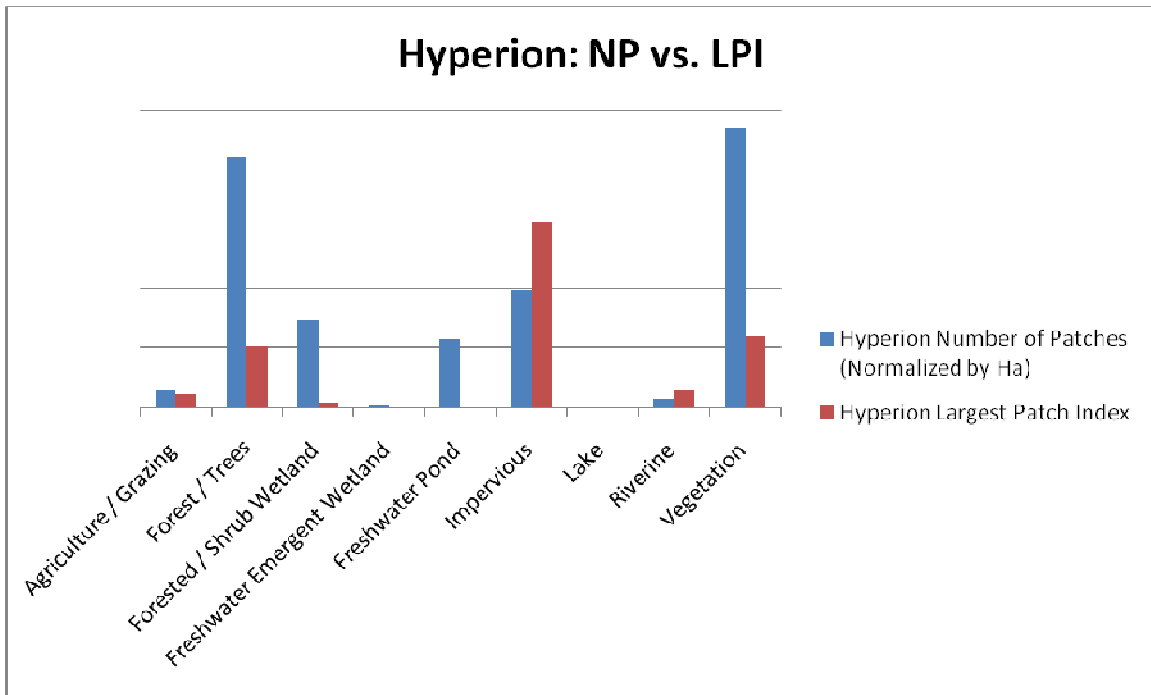


Figure 32. Hyperion Number of Patches and Largest Patch Index per Class Comparison

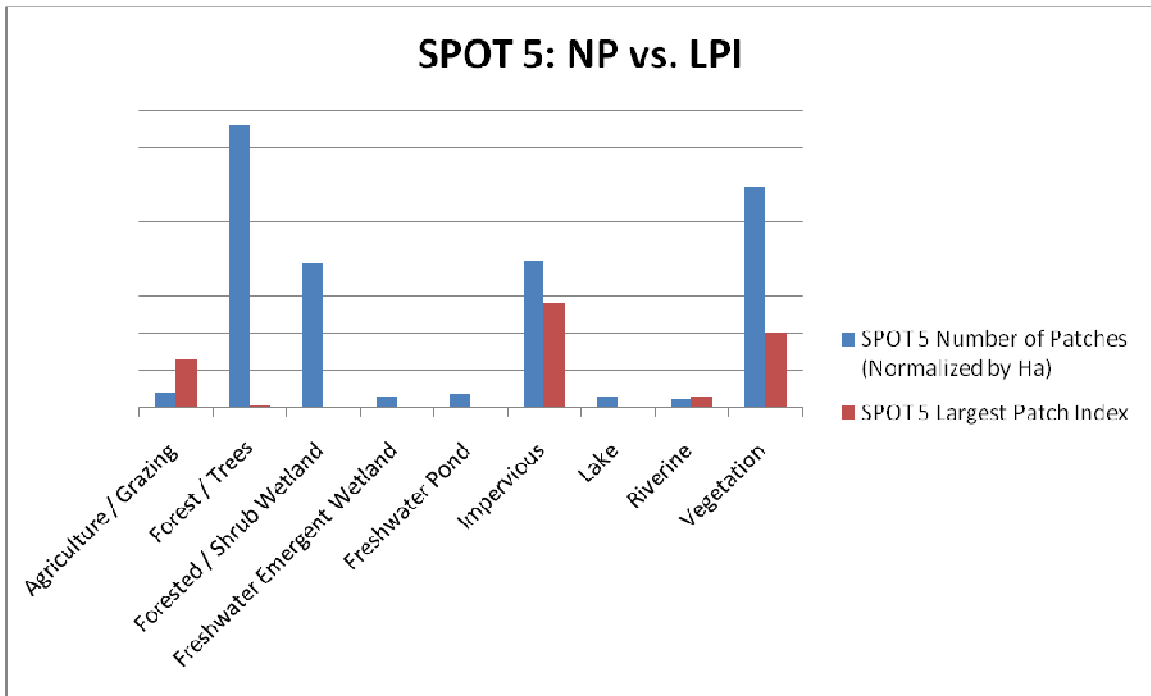


Figure 33. SPOT 5 Number of Patches and Largest Patch Index per Class Comparison

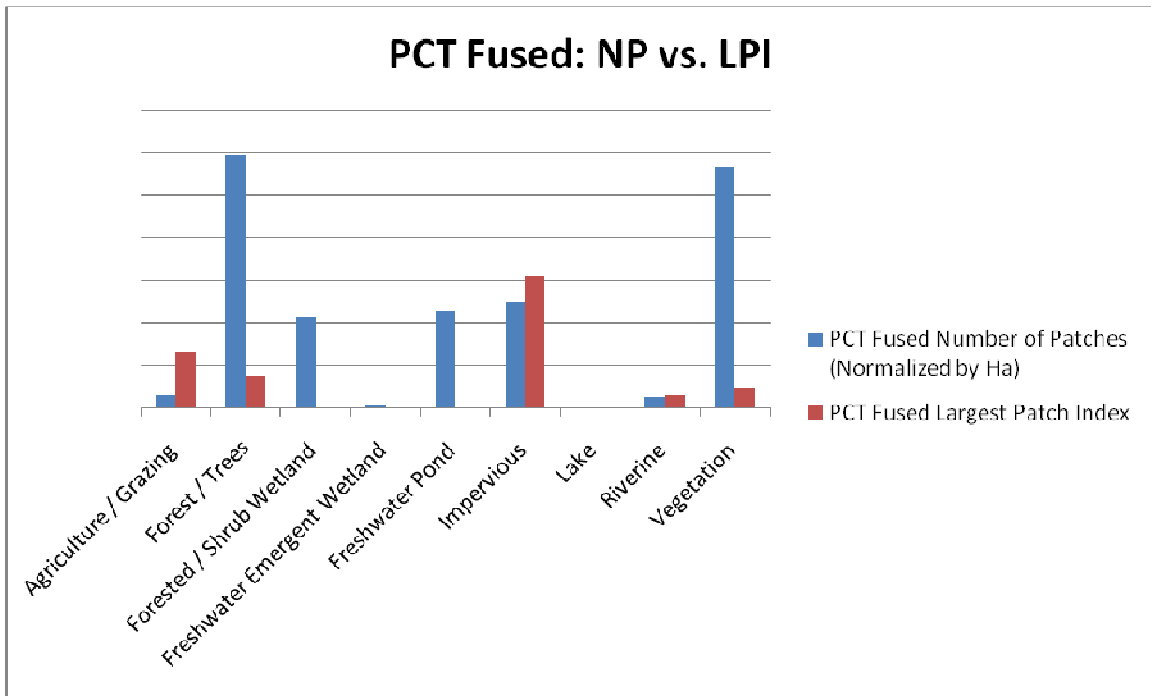


Figure 34. PCT Fused Number of Patches and Largest Patch Index per Class

Comparison

It is also clear from the preceding charts that spatial resolution directly impacts the comparison between these two metrics. This is especially clear in the Forest / Trees class, the Impervious class, and the Agriculture / Grazing class. The SPOT 5 and PCT fused datasets show that the largest patch index was greater than the number of patches over the lower spatial resolution Hyperion dataset for the Agriculture / Grazing class.

The Hyperion and PCT fused datasets indicate that the largest patch index was less than the number of patches over the lower spectral resolution SPOT 5 dataset for the Impervious class. The Hyperion and PCT fused datasets also indicated a higher total for

the largest patch index than the SPOT 5 dataset, while all three datasets still had a largest patch index much lower than the number of patches metric.

The correlation coefficient was calculated for the results from the largest patch index, class area, and number of patches metrics using Microsoft Excel (Equation 12).

$$Correlation(x, y) = \frac{\sum (x - \bar{x})(y - \bar{y})}{\sqrt{\sum (x - \bar{x})^2 \sum (y - \bar{y})^2}}$$

Equation 12. Correlation Between Arrays X and Y

Correlation was computed between the pairs of the SPOT 5 – PCT fused datasets, the Hyperion – PCT fused datasets, and the Hyperion - SPOT 5 datasets. The results show moderately high correlation between each pair of datasets. Regarding the largest patch index, the SPOT 5 – PCT fused correlation and Hyperion – SPOT 5 correlation each totaled 0.84, while the Hyperion – PCT fused dataset correlation was highest at 0.89. The class area showed similar results with the SPOT 5 – PCT fused and Hyperion – SPOT 5 correlations each totaling 0.97, while the Hyperion – PCT fused dataset correlation was highest at 0.99. The number of patches metric showed identical results with correlations for all three pairs totaling to 0.93. The very minor difference in correlations between pairs suggest that all three datasets performed similarly. However, the PCT fused dataset’s constant involvement with the more highly correlated pairs coupled with the best overall accuracy suggests that this was the best performing dataset.

Further calculations to test the connectivity or fragmentation of the classified landscapes included Contagion, Shannon's Diversity Index, and Shannon's Evenness Index. In all three datasets, very similar results were found in all three of these metrics. Regarding Contagion, the Hyperion, SPOT 5, and PCT fused datasets had contagion values of 50.92%, 48.90%, and 50.42% respectively. These results indicate that the patches within the landscapes were not extremely aggregated or diagggregated; thus, there is a slight level of fragmentation found within all the classified landscapes. Shannon's Diversity Index indicated values of 1.45, 1.47, and 1.50 for each classified dataset respectively. These values appear low, but there is no limit to what these values could reach. The most diverse landscape was derived from the PCT fused dataset, caused by both enhance spatial and spectral characteristics of the underlying dataset affected the classified patch results. Shannon's Evenness Index is normalized by the number of patches found in each dataset, giving an output range from 0 – 1. These results agreed with the contagion results suggesting a moderately evenly dispersed landscape within each dataset, with values of 0.58, 0.59, and 0.59 respectively.

CHAPTER 6

SUMMARY AND CONCLUSION

This study focused on the ability to meaningfully classify differing wetland types with similar classification schemes to that of the NWI datasets produced in the 1980's by the United States Department of Fish and Wildlife with low-cost multispectral and hyperspectral imagery. The results from this study indicate that it is possible to obtain better classification results, yielding more informative landscape metrics, by fusing low spatial resolution hyperspectral imagery with high spatial resolution multispectral imagery. The PCT fused imagery resulted in the best overall accuracy of 88%, totaling 8% higher than the least accurate SPOT 5 dataset at 80%. While the SPOT 5 dataset produced very good individual class results, which in some cases exceeded that of individual class accuracies for the PCT fused dataset, the PCT fused dataset maintained better accuracies for classes such as Freshwater Emergent Wetland, Forested / Shrub Wetland, and open water classes. Considering that these were primary drivers for this study, the PCT fused dataset produced the best results out of all three tests.

The classification methodology for this study was a very detailed approach on exploiting digital image information. There are many other methodologies that could be employed, but highly detailed hyperspectral analysis techniques allow the ability to dissect digital imagery in a more intensive manner. While atmospheric correction is generally always performed with hyperspectral analysis, it is not always necessary with multispectral analysis. Performing atmospheric correction on the multispectral dataset

converted raw digital numbers within the data to reflectance, allowing a more detailed comparison of class spectra when viewing the spectral profiles developed from class end-members. Unlike hyperspectral datasets, derivative analysis is not possible with multispectral data due to lacking detail in the derived dataset spectral signatures. Despite this, other detailed hyperspectral methodology employed with the multispectral SPOT 5 dataset was still employed as an enhanced mapping technique. The SAM and MF approaches are far stricter when classifying either hyper – or multispectral imagery than more conventional classification algorithms.

The metrics calculated in this study also indicated that the PCT fused dataset resulted in more meaningful results. Enhanced spatial and spectral resolution of this dataset allowed better segregation of spectrally similar features within the landscape, and better defined edges between neighboring patch types. This was clear in the Forested / Shrub Wetland class, where the Hyperion dataset appeared to have difficulties in finding patch boundaries due to coarse spatial resolution. After fusing the high spatial resolution with high spectral resolution, there was a class accuracy increase of 8%, and a decrease in both class area and number of patches. Based on ancillary datasets, these results seemed far more accurate within this study area. Open water classes, Lake and Freshwater Pond had far better class accuracies. It was clear that the SPOT 5 dataset constantly misclassified impervious features as open water and vice versa due to spectral similarities. Both Hyperion and PCT fused datasets performed far better on these classes which is noticeable with similar metrics; however, the PCT fused dataset had more clearly defined edges allowing more meaningful resulting metrics.

Classification results and metrics analysis in this study showed the definite advantages of using hyperspectral imagery to classify and quantify landscapes that contain moderate to high class heterogeneity. Furthermore, the results from this study also indicate that spatial resolution is of the utmost importance when trying to classify landscapes that would likely contain relatively small or narrow features of interest; in particular, long narrow rivers, relatively small ponds, etc. Very spectrally similar features in this study, such as dense forests and forested emergent wetlands, were classified with greater success when using the PCT fused hyperspectral dataset. These classes were still difficult to separate due to similar composition, but it remained clear that the narrow band spacing of the hyperspectral imagery allowed the ability to better distinguish between the two.

Recommendations for Further Research

The more detailed edges found for all classes derived within the PCT fused dataset ultimately displayed that higher spectral and spatial resolution datasets are ideal for wetland mapping. This methodology was a cost effective approach to take advantage of both higher spectral and spatial resolution considering these types of datasets are now currently available at little to no cost. The EO-1 satellite is equipped with both the Hyperion sensor and an additional sensor and the Advanced Land Imaging (ALI) sensor. The ALI sensor's specifications include 7 multispectral bands with 30m resolution, as well as a 10m resolution panchromatic band. Effective August 5, 2009 the USGS Earth

Resources Observation and Science (EROS) Center announced that future data access requests for new imagery on-board the EO-1 satellite will be processed at no charge. This allows the ability to obtain hyperspectral and multispectral / panchromatic imagery at the same time; thus, the higher resolution panchromatic imagery will cover the exact area as the hyperspectral imagery, as well as ensuring no landscape changes between datasets exist. The relationship between PCT fused hyperspectral outputs and the panchromatic image captured at the same time would allow for less distortion between the datasets and could create a better product than what was resultant from this study.

With these datasets no longer costing thousands of dollars to purchase, cities, metros, counties, or even states could be mapped with this type of imagery without looming extensive costs. While this would be an immense amount of processing and time commitment, ENVI IDL programming could easily be performed to batch most of the preprocessing, and post processing steps involved. It is not uncommon for hyperspectral analysis projects to require tens to hundreds of flight lines from intrinsically large study sites with higher spatial resolution. Utilizing the methods performed in this study would reduce the number scan lines necessary to cover a larger study area, while only sacrificing a small amount of spatial resolution from aerial hyperspectral imagery that is obtained for tens to hundreds of thousands of dollars.

Additionally, time series research for larger study areas may be performed with this study's methodology. Such research could indicate landscape change with greater regards to wetland areas, endangered species, etc. Furthermore, inferences could be made about how local population growth, increasing upland impervious area, storm water

runoff, and other urban expansion activities are affecting the wetlands surrounding them, as well as the migration patterns of the fish and wildlife that utilize these areas as their natural habitats. Invasive species could be mapped within urban wetlands, and correlations between this and land use change could be tested. Additionally, coupling such research with urban heat island analysis could allow inferences on how the landscape and wetlands within an urban area are affecting or being affected by increasing temperatures.

APPENDIX A

Accuracy Assessment Tables

Hyperion (30m)											
Classification	Reference										
	Agriculture / Grazing	Forest / Trees	Forested / Shrub Wetland	Freshwater Emergent Wetland	Freshwater Pond	ImperVIOUS	Lake	Riverine	Vegetation	Total	Class Accuracy
Agriculture / Grazing	45	1				2			2	50	90%
Forest / Trees		43	4	1					2	50	86%
Forested / Shrub Wetland		10	40							50	80%
Freshwater Emergent Wetland	1	5	1	35		2		6		50	70%
Freshwater Pond				1	46	1		2		50	92%
ImperVIOUS		1			3	42		2		50	84%
Lake				6			44			50	88%
Riverine					1	2		47		50	94%
Vegetation	2	3	1	1		1		42		50	84%
	48	63	46	44	50	50	44	51	54	450	85%

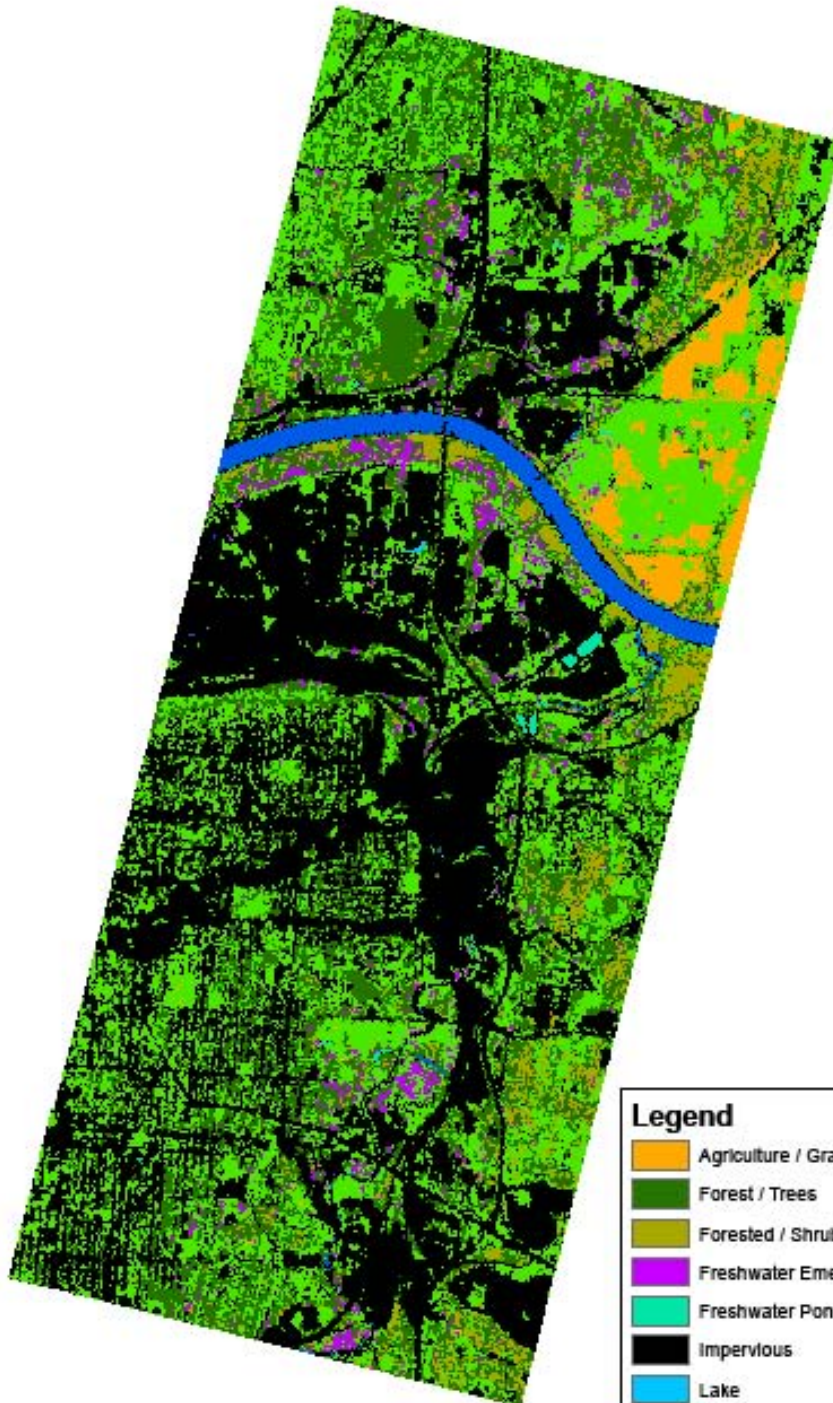
SPOT 5		Reference											
Classification	Agriculture / Grazing	Forest / Trees	Forested / Shrub Wetland	Freshwater Emergent Wetland	Freshwater Pond	Impervious	Lake	Riverine	Vegetation	Total	Class Accuracy		
Agriculture / Grazing	49				1					50	98%		
Forest / Trees		43	2			3			2	50	86%		
Forested / Shrub Wetland		10	37	1		2				50	74%		
Freshwater Emergent Wetland		3		37		9			1	50	74%		
Freshwater Pond				1	32	16				50	64%		
Impervious	2					47				50	94%		
Lake					1	21	24		2	50	48%		
Riverine							2	48		50	96%		
Vegetation	1	2	2	3					42	50	84%		
	52	58	41	43	33	98	26	52	47	450	80%		

Principal Components Transformation - Fused		Reference											Total	Class Accuracy
Classification	Agriculture / Grazing	Forest / Trees	Forested / Shrub Wetland	Freshwater Emergent Wetland	Freshwater Pond	Impervious	Lake	Riverine	Vegetation					
Agriculture / Grazing	47	46	1	3		1							50	94%
Forest / Trees		6	42	2		1			1				50	92%
Forested / Shrub Wetland		2	3	39		6			5				50	78%
Freshwater Emergent Wetland	1			1	41	49			2				50	82%
Freshwater Pond					1	6			2				50	98%
Impervious						1	40						50	80%
Lake				1	2			7					50	96%
Riverine			1			1		48					50	96%
Vegetation	1	2		1					46				50	92%
	49	56	47	47	44	58	40	55	54				450	88%

APPENDIX B

Land Cover Classification Maps

Hyperion Land Cover Map



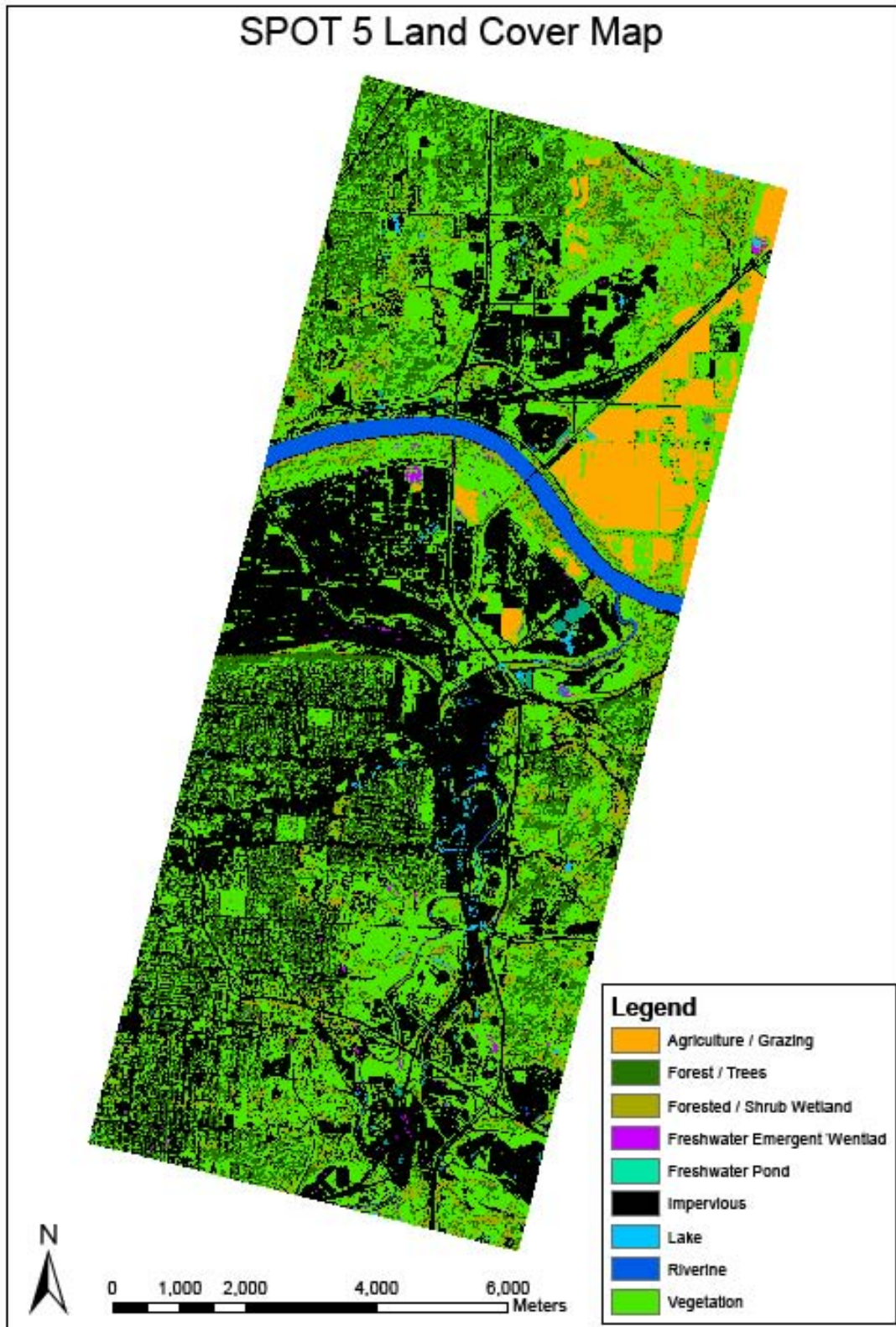
Legend

- Agriculture / Grazing
- Forest / Trees
- Forested / Shrub Wetland
- Freshwater Emergent Wetland
- Freshwater Pond
- Impervious
- Lake
- Riverine
- Vegetation

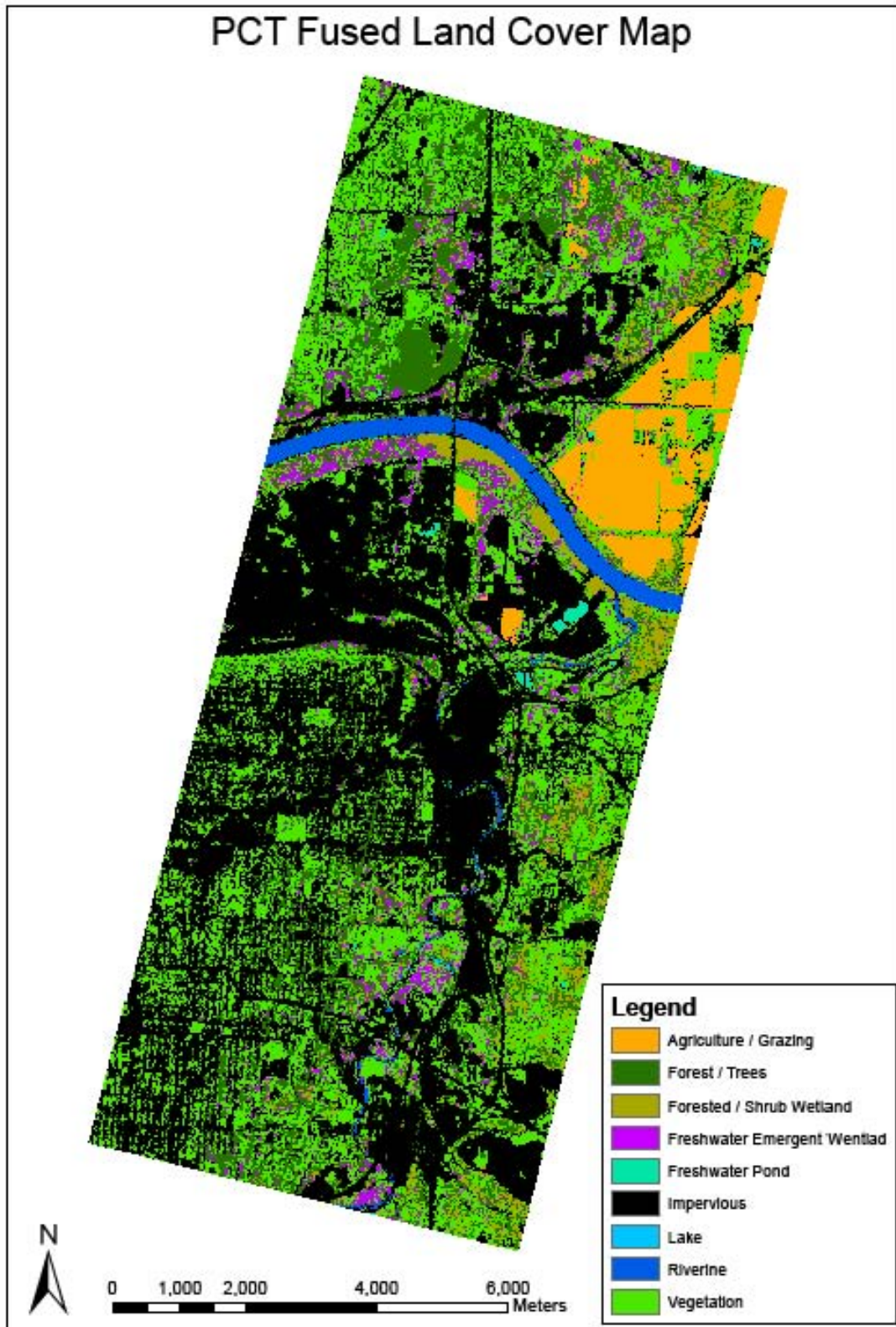


0 1,000 2,000 4,000 6,000 Meters

SPOT 5 Land Cover Map



PCT Fused Land Cover Map



REFERENCE LIST

- Artigas, F. J., and Yang, J. 2004. Hyperspectral remote sensing of habitat heterogeneity between tide-restricted and tide-open areas in the New Jersey Meadowlands. *Urban Habitats*, 2(1): 112 -114.
- Carrão, H., and Caetano, M. The effect of scale on landscape metrics. Paper presented at the International Society for Remote Sensing of the Environment conference, Buenos Aires, Argentina, 8 – 12 April 2002.
- Corry, R. C., and Laforteza, R. 2007. Sensitivity of landscape measurements to changing grain size for fine-scale design and management. *Landscape Ecological Engineering*, 3: 47 – 53.
- Beck, R. 2000. EO-1 user guide. University of Cincinnati, Version 2.3;
< <http://eo1.usgs.gov/documents.php>>
- Darvishi, A., Kappas, M., and Erasmi, S. Hyper-spectral/high-resolution data fusion: assessing the quality of EO1-Hyperion/Spot-Pan & Quickbird-MS fused images in spectral domain. Paper presented at the International Society for Photogrammetry and Remote Sensing Workshop, Hannover, Germany, 17 – 20 May 2005.
- Enger, E. D., and Smith, B. 2004. *Environmental science: a study of interrelationships*. 9th ed. Boston: Mc Graw – Hill Higher Education.
- Ehrenfeld, J. G. 2000. Evaluating wetlands within an urban context. *Ecological Engineering*, 15: 253 – 265.

- Fuller, L.M., Morgan, T. R., and Aichele, S. S. 2006. *Wetland delineation with IKONOS high-resolution satellite imagery, Fort Custer Training Center, Battle Creek, Michigan, 2005*: U.S. Geological Survey, Scientific Investigations Report 2006-5051.
- Gergel, S. E., and Turner, M. G. 2002. *Learning landscape ecology: a practical guide to concepts and techniques*. New York: Springer Science + Business Media, LLC.
- Grayson, J.E., Chapman, M. G., and Underwood, A. J. 1999. The assessment of restoration of habitat in urban wetlands. *Landscape and Urban Planning*, 43: 228.
- Green, A. A., Berman, M., Switzer, P., and Craig, M.D. 1988. A transformation for ordering multispectral data in terms of image quality with implications for noise removal. *IEEE Transactions on Geoscience and Remote Sensing*, 26(1): 65-74.
- ITT Visual Information Solutions. 2006. ENVI user's guide: basic tools. Boulder, Colorado: ITT Visual Information Solutions.
- Ji, W. 2008. Landscape effects of urban sprawl: Spatial and temporal analyses using remote sensing images and landscape metrics. *The International Archives of the Photogrammetry, Remote Sensing and Spatial Information Sciences*, 37(B7): 1691-1694.
- Jollineau, M. Y., and Howarth, P. J. 2008. Mapping an inland wetland complex using hyperspectral imagery. *International Journal of Remote Sensing*, 29(12): 3609 – 3631.

- McClary Jr., M. 2004. *Spartina alterniflora* and *Phragmites australis* as habitat for the ribbed mussel, *Geukensia demissa* (Dillwyn), in Saw Mill of New Jersey's Hackensack Meadowlands. *Urban Habitats*, 2(1): 83 - 85.
- McGarigal, K., Cushman, S. A., Neel, M. C., and Ene, E. 2002. FRAGSTATS: spatial pattern analysis program for categorical maps. Computer software program produced by the authors at the University of Massachusetts, Amherst. Available at the following web site:
<http://www.umass.edu/landeco/research/fragstats/fragstats.html>
- Ozesmi, S. L., and Bauer, M. E. 2002. Satellite remote sensing of wetlands. *Wetlands Ecology and Management*, 10: 381 – 402.
- Pande, H., Tiwari, P. S., and Dobhal, S. 2009. Analyzing hyper-spectral and multi-spectral data fusion in spectral domain. *Indian Society of Remote Sensing*, 37: 395 – 408.
- Rouse, K. 2004. *Final report to the U.S. Environmental Protection Agency, Region 7: assessing urban wetlands*. Water Resources Program, Geological Survey and Resource Assessment Division; Missouri Department of Natural Resources.
- Salem, G., Kafatos, M., El-Ghazawi, T., Gomez, R., and Yang, R. 2005. Hyperspectral image assessment of oil-contaminated wetland. *International Journal of Remote Sensing*, 26(4): 811 – 821.
- Strang, G. 2005. *Introduction to Linear Algebra*. 3rd ed. Wellesley: Wellesley – Cambridge Press.

- Sun, Y., Liu, X., and Liao, C. 2008. Identifying hyperspectral characters of wetland species Using in-situ data. *The International Archives of the Photogrammetry, Remote Sensing and Spatial Information Sciences*, 37(B7): 459 – 466.
- Townsend, P. A., and Walsh, S. J. 2001. Remote sensing of forested wetlands: application of multitemporal and multispectral satellite imagery to determine plant community composition and structure in southeastern USA. *Plant Ecology*, 157: 129 – 149.
- Turner, M. G., Gardner, R. H., and O'Neill, R. V. 2001. *Landscape ecology in theory and practice: pattern and process*. New York: Springer Science + Business Media, LLC.
- Windham, L., Laska, M. S., and Wollenberg, J. 2004. Evaluating urban wetland restorations: case studies for assessing connectivity and function. *Urban Habitats*, 2(1): 130 – 131.

VITA

Daniel W. Gwartney was born August 24, 1981 in the state of Kansas. After graduating from Rockhurst High School, Kansas City, MO in 2000, he attended the University of Kansas as a full time undergraduate student in the Department of Geography. At the University of Kansas, he worked for one year with the Kansas Applied Remote Sensing project under Professors Kevin Price and Stephen Egbert as a student research assistant. He graduated with the class of 2006 earning a Bachelor's of Science in Geography with an emphasis on GIS and Remote Sensing, as well as earning a minor in Atmospheric Science. In 2006, he began working as a GIS Analyst with AMEC Earth and Environmental.

In 2008, he began fulfilling requirements for a Master's of Science degree in Urban and Environmental Geosciences with an emphasis in urban and environmental geography and GIS. While completing these requirements, he continued full-time employment with AMEC Earth and Environmental, helping build capabilities and strength within the field of remote sensing. He co-authored a report entitled Using LiDAR for Structure Inventory and Enhanced Terrain Model Development, and presented findings at the Floodplain Managers Conference in San Diego, CA.

Upon completion of his Masters of Science requirements, he plans on continuing employment with AMEC Earth and Environmental as a Remote Sensing Scientist, as well as pursuing a doctorate in the environmental remote sensing.